A Riemannian Distance in Signal Design for MIMO Radar

A RIEMANNIAN DISTANCE IN SIGNAL DESIGN FOR MIMO RADAR

BY

JIA XU, B.Sc., (Electrical Engineering)

Beijing Institute of Technology, Beijing, China

A THESIS

SUBMITTED TO THE DEPARTMENT OF ELECTRICAL & COMPUTER ENGINEERING

AND THE SCHOOL OF GRADUATE STUDIES

OF MCMASTER UNIVERSITY

IN PARTIAL FULFILMENT OF THE REQUIREMENTS

FOR THE DEGREE OF

MASTER OF APPLIED SCIENCE

Master of Applied Science (2014) McMaster University

(Electrical & Computer Engineering) Hamilton, Ontario, Canada

TITLE:	A Riemannian Distance in Signal Design for MIMO Radar
AUTHOR:	Jia Xu M.Sc., (Electrical Engineering) Columbia University, New York, U.S.A. B.Sc., (Electrical Engineering) Beijing Institute of Technology, Beijing, China
SUPERVISOR:	Dr. K. M. Wong, Dr. T. N. Davidson
NUMBER OF PAGES:	xi, 72

To my parents and my friends

Abstract

We examine the signal design for Multiple Input Multiple Output (MIMO) radar by matching a desired beam pattern, while suppressing the auto-correlation and cross-correlation sidelobes. We further reason that since the estimated covariance matrix of the transmitted signal forms a manifold in the signal space, the difference between the estimated covariance matrix and the desired one should be measured in terms of Riemannian distance (RD) instead of the commonly used Euclidean Distance (ED). We transform the design problem into a convex (CVX) optimization problem which can be solved efficiently by convex optimization methods. Applying RD concept of measure to our design objective function, results show that the performance of our design is superior to that of using ED for the objective.

Acknowledgements

I would like to express my sincere thankfulness to all those people who have given me great help in pursuing the degree of Master of Applied Science at McMaster University for these two years, as well as in completing my thesis.

First and foremost, I would like to give my heartfelt gratitude to one of my supervisors, Dr. Kon Max Wong for his advisable suggestions, ingenious commitment, inspiring ideas and continuous encouragement, which have let me know the right direction of my study and research.

Secondly, I really appreciate the guidance and help from the other supervisor of mine, Dr. Tim Davidson, without whom I can not progress the research and solve its problems easily.

Besides, I would like to thank my parents, who give me generous and continuous support whenever and wherever. Without them, I can not make my current achievements.

Finally, I want to thank my friends who have always been a constant source of courage and inspiration to me.

Notation and Abbreviations

Notations

$\mathbf{A}$	Matrices
$\mathbf{a}$	Vectors
$(\cdot)^T$	Matrix transpose
$(\cdot)^{-1}$	Matrix inverse
$(\cdot)^\dagger$	Matrix pseudo inverse
$(\cdot)^*$	Matrix complex conjugate
$(\cdot)^H$	Matrix hermitian
$\text{diag}\{\cdot\}$	Diagonal matrix
$\mathbf{I}_N$	$N \times N$ identity matrix
$\mathbb{R}$	Field of real numbers
$\mathbb{C}$	Field of complex numbers
$\text{tr}(\cdot)$	Trace of matrices
$\mathbf{0}$	Zero matrices
$\mathbf{A} \succeq \mathbf{B}$	$\mathbf{A}$, $\mathbf{B}$ and $\mathbf{A} - \mathbf{B}$ are all positive semi-definite matrices
$[\mathbf{A}]_{ij}$	The entry in the ith row and jth column
$\mathcal{M}$	Manifold

$\otimes$	Kronecker product
δ_{kl}	Kronecker delta: 1, if $k = l$; otherwise 0
$\|\| \cdot \|\|$	Frobenious norm of a vector or a matrix
$\langle \cdot \rangle$	Inner product

Abbreviations

ED	Euclidean Distance
i.i.d.	Independent and Identically Distributed
FN	Frobenius Norm
ISI	Inter-symbol Interference
MIMO	Multiple Input Multiple Output
MISO	Multiple Input Single Output
N-D	N Dimensional
PSD	Positive Semidefinite
RD	Riemannian Distance
SIMO	Single Input Multiple Ouput
SISO	Single In Single Out
SNR	Signal to Noise Ratio

Contents

List of Figures

Chapter 1

Introduction

1.1 A Radar System

A radar system employs electromagnetic waves to detect distant objects and, from the returned waves, to estimate the parameters of these targets, which usually are aircraft, ships, vehicles, people, meteorological events, or terrains. The parameters of these targeted objects include locations, directions and velocities of movements [6]. Figure 1.1 shows the major processing elements involved in a radar system. These include the processes of transmitting a radar signal, propagation of the signal through the atmosphere, reflection of the signal from the target, and receiving the reflected signals.

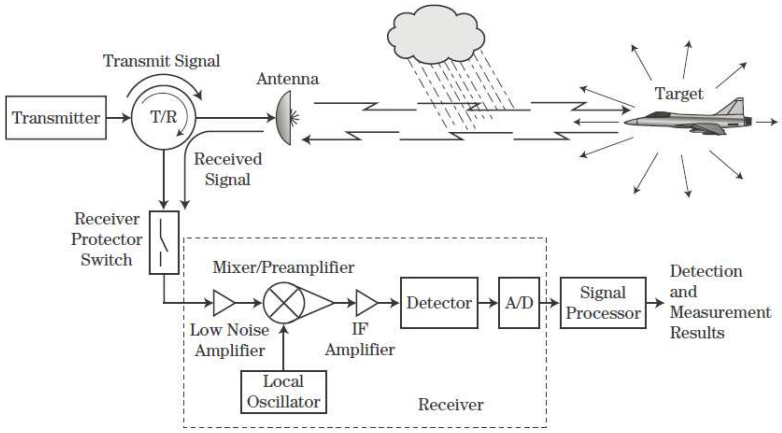

Figure 1.1: Illustration of a Radar System [1]

The major parts in a radar system include a transmitter, an antenna, a receiver and a signal processor. The subsystem that generates electromagnetic waves is the transmitter. The antenna takes these electromagnetic waves as input from the transmitter and passes them into the propagation medium. The transmitter is connected to the antenna through a transmission/reception (T/R) device, which has the function of providing a connection point so that the transmitter and the receiver can both be attached to the antenna. The transmitted signal propagates through the medium to the target. In this propagation process, the electromagnetic waves induce currents on the target, which reradiate waves back into the environment. In addition to the desired target, other surfaces on the ground or in the atmosphere reflect the signal. Some of the reradiated signals from objects including the target propagate towards the receiver. Propagation effects of the atmosphere and the earth on these waves may alter the strength of the electromagnetic waves both at the target and at the receive antenna. The receiver antenna captures the electromagnetic waves reflected from the

object, which are passed to the receiver circuits. The components in the receiver amplify the received signal, convert the radio frequency signal to an intermediate frequency, and subsequently apply the signal to an analog-to-digital converter (ADC). The detector is the device that removes the carrier from the modulated return signal so that target data can be analyzed by the signal processor. A primary function of the radar signal processor is to determine the presence of a target in the presence of interference, such as noise, clutter and jamming [1].

1.2 From SISO to MIMO Radars

Radar systems have evolved through different generations, from Single Input Single Output (SISO) to Multiple Input Multiple Output (MIMO). In the SISO systems, the transmitter operates with one antenna, as does the receiver. Therefore, there is no diversity and no additional processing required. The advantage of a SISO system is its simplicity. However, SISO systems are limited in their performance. The system will be more easily affected by interference and fading than other advanced systems. When an electromagnetic wave interacts with other obstacles, the reflected waveforms may become scattered and take many paths to reach the receiver. This multipath issue can cause fading, losses and attenuation, etc. [7]. Another type of radar is the phased array radar. The system can only transmit scaled versions of a single waveform, which are perfectly correlated. Because only a single waveform is used, the phased array radar is also called single input multiple-output (SIMO) radar and is known as receive diversity [6]. A MIMO radar is a generalization of a phased array in that the signals need not be correlated from one antenna element to another. Figure 1.2 and Figure 1.3 [2] are brief illustrations of phased-array radar and MIMO radar. It is

characterized by its ability to emit signals from multiple spatially diverse transmission antenna elements and to observe the returns from multiple spatially diverse reception element [8], although the signals may or may not be correlated. In much of the current literature, the waveforms transmitted from each antenna are assumed to be orthogonal, but this is not a requirement for MIMO radar. However, orthogonality facilitates the subsequent processing of the received signals. MIMO radar systems have many potential advantages, such as improved target detection performance, enhanced angle estimation accuracy, and decreased minimum detectible velocity [6]. For statistical MIMO radar, in which the transmission and reception antenna elements are broadly separated, providing independent scattering responses for each antenna pairing, the diversity provided by the multiplicity of transmission and reception angles can be exploited to improve the detection performance. Moreover, spatial diversity can be employed to reduce the probability of a bad scattering response causing a target to be missed [9]. Coherent MIMO radar is another type of MIMO radar, in which the transmission and reception array elements are closely spaced so that the target is in the far field of the transmission-reception array. In this radar system, since the antennas are spaced relatively closely to each other, angle estimation performance can be enhanced. In some sense, the performance of the MIMO system can be characterized by a virtual array constructed by the convolution of the transmission and reception antenna locations. This virtual array can be much larger than the one of an equivalent traditional system [9]. Thus, the MIMO system will have much better intrinsic resolution. Above all, fully exploiting the potential of MIMO radar systems can result in more significantly improved target detection and tracking, parameter estimation, and recognition performance than other radar systems.

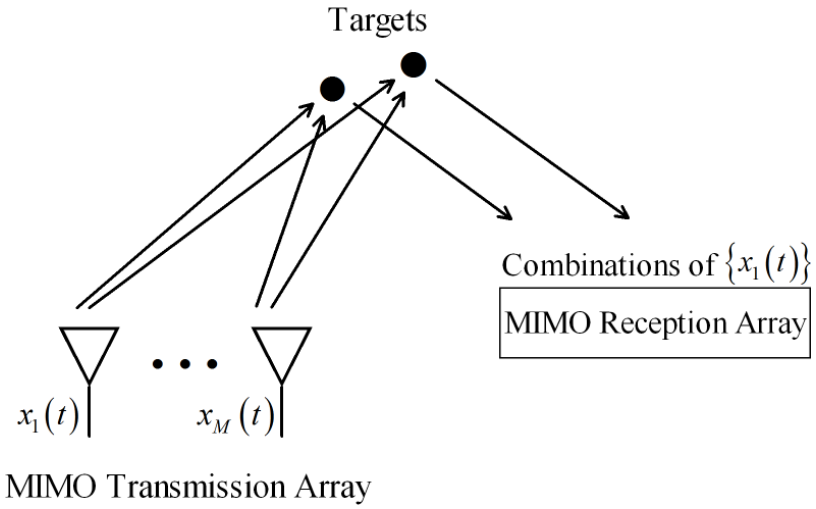

Figure 1.2: MIMO Radar [2]

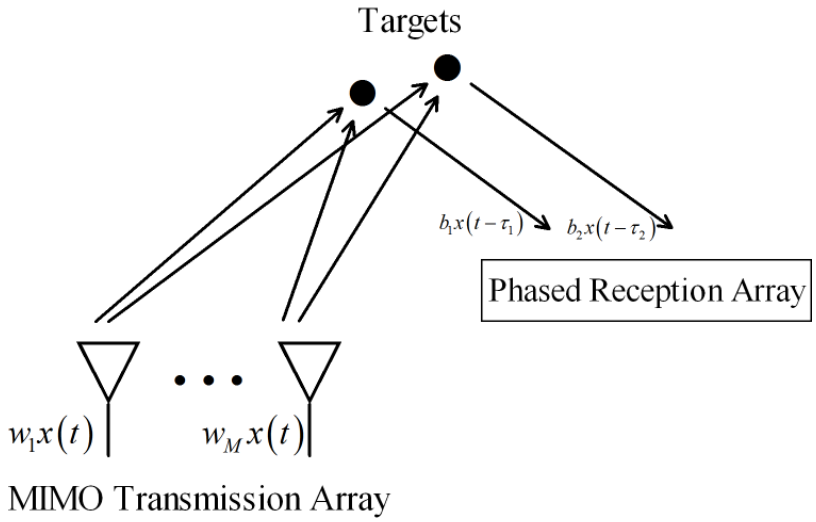

Figure 1.3: Phased-Array Radar [2]

1.3 Signal Design in MIMO Radar

In recent years, the field of MIMO radar has been developing rapidly. Along with the rapid development, the design of incoherent waveforms for each of the transmitting antennas has drawn considerable attention from researchers. Extensive methods and algorithms about signal design for MIMO radar are proposed, which aim at matching a given transmission beampattern [10]. Radar analysis and radar signal design problems have also been examined from the point of information theory [11, 12]. Ensuing research in radar signal design inspired by this approach includes [13, 14, 15] which are carried out by maximizing the mutual information (MI) between the target impulse response and the reflected radar waveforms. Chen and Vaidyanathan [16] extend the radar ambiguity function to MIMO radar which characterizes the resolutions of the radar system, and aims at reducing the sidelobes of the MIMO radar in terms of ambiguity function. However, most of the research in transmitted waveform design for MIMO radar is concerned with how to design these waveforms so that they possess a desired covariance matrix $\mathbf{R}$. Stoica et al. [17] optimized the covariance matrix of the transmitted waveforms to achieve a given transmission beampattern, and modified the beampattern matching criterion in terms of the cross-correlation between the signals bounced back to the radar from the targets of interest. Wang et al. [5] presented the design of unimodular signal sets with good orthogonal, auto-correlation and cross-correlation properties using different algorithms. Here, the signal waveforms are optimized to meet the beam pattern specification directly by formulating the problem as an unconstrained fourth-order trigonometric polynomial minimization model. A quasi-Newton iterative algorithm is implemented to solve it. Similarly, in [4], the waveforms were also synthesized directly to approximate a given covariance

matrix by deploying a cyclic algorithm (CA). However, the signal waveform matrix was reformulated into a larger one, which could hardly satisfy the signals with a long lasting period. He et al. [3] introduced several CAs for unimodular waveform design by transforming existing problem into different mathematical expressions.

1.4 Contribution of This Thesis

In the above-mentioned methods of synthesizing signals, the treatment of the errors in the estimation of covariance matrices is usually in terms of the *Euclidean Distance* (ED), which is induced by the corresponding inner product norm for matrices, called the *Frobenius Norm* (FN). The use of the ED might not be appropriate for modeling the mismatch on the covariance matrices since the covarince matrices are not freely structured, but are *Hermitian and positive semi-definite* (PSD). Therefore, the set of covariance matrices forms a *manifold* in the signal space. Thus, instead of using the *Frobenius Norm*, the distance between the true covariance matrix $\mathbf{R}$ and the estimated covariance matrix $\hat{\mathbf{R}}$ should be measured more appropriately along the surface of the manifold using a *Riemannian Distance* (RD) [18]. This concept is akin to finding the distance between two cities on Earth: The ED between two cities is neither informative nor accurate.

In this thesis, we employ the RD for measuring the estimation error in the covariance matrix instead of using the ED metric. The goal of our design is to attain the transmitted signal directly rather than decomposing the estimated covariance matrix to obtain the desired signal. To further guarantee the properties of incoherent waveforms, we define auto-correlation and cross-correlation constraints in this problem. An iterative approach is used to approximate the original problem. In each iteration,

aspects of the design obtained in the previous iteration are employed to drive the algorithm, until the predefined convergence criteria are satisfied. We also show how the proposed approach can be used to design signals using the ED metric.

1.5 Outline of the Thesis

In this thesis, we propose to design the transmitted signals to meet certain specifications directly using RD. In Chapter 1, the background knowledge of MIMO radar and the contribution of our work are briefly introduced. In Chapter 2, we introduce some existing researches on MIMO radar signal design mainly from three approaches. Including the MIMO radar signal model and statistical properties, all of these will be discussed in details in this chapter. Our proposed method using RD as an error measure is introduced in Chapter 3. A brief introduction of RD is provided. Model formulation and the iterative method used to transform our problem into a convex one are also given in this chapter. Numerical results are shown in Chapter 4. Finally, the conclusion of this thesis and our future work are presented in Chapter 5.

Chapter 2

Signal Design Methods in MIMO Radar

The MIMO radar transmitting orthogonal waveforms benefits from the waveform diversity to extract useful information at a receiver via the use of different waveforms [19]. In recent years, most of the research on waveform design for MIMO radar has taken an algorithmic approach. In this chapter, we will review three approaches: two Cyclic Algorithms (CAs) and one Quasi-Newton Algorithm. All these are designed to match a desired covariance matrix with Euclidean Distance (ED).

2.1 Multiple Input Multiple Output (MIMO) Signal Model

Consider that a MIMO radar system consists of M_t transmission antennas and M_r reception antennas. To simplify the notation, we assume that the numbers of antennas

in the transmitter and in the receiver are both equal to M. Let $x_m(n)$ denote the discrete time baseband signal transmitted by the mth antenna at time slot n, and define

$$\mathbf{x}_m = [x_m(1), x_m(2), \ldots, x_m(N)], \text{ with } 1 \leq m \leq M,$$
$$\mathbf{x}(n) = [x_1(n), x_2(n), \ldots, x_M(n)]^T, \text{ with } n = 1, \ \ldots, \ N,$$

where $\mathbf{x}_m$ represents the transmitted signal sequence from the mth antenna, N denotes the number of samples in each waveform [17], and $\mathbf{x}(n)$ denotes the vector of transmitted signals at time n.

We will construct $\mathbf{X}$ so that it consists of the transmitted signals from all the antennas, such that

$$\begin{aligned}\mathbf{X} &= [\mathbf{x}_1, \mathbf{x}_2, \ldots, \mathbf{x}_M]^T \\ &= \begin{bmatrix} x_1(1) & x_1(2) & \ldots & x_1(N) \\ x_2(1) & x_2(2) & \ldots & x_2(N) \\ \vdots & \vdots & \ddots & \vdots \\ x_M(1) & x_M(2) & \ldots & x_M(N) \end{bmatrix}, \text{ with } \mathbf{X} \in \mathbb{C}^{M \times N}.\end{aligned} \tag{2.1}$$

Let θ_k denote the location parameter of the kth generic target, and then the transmitting steering vector is

$$\mathbf{a}(\theta_k) = [e^{j2\pi f_0 t_1(\theta_k)}, e^{j2\pi f_0 t_2(\theta_k)}, \ldots, e^{j2\pi f_0 t_M(\theta_k)}]^T,$$

where $t_m(\theta_k)$ is the time needed by the signal emitted via the mth transmission antenna to arrive at the target located at θ_k.

Here, we are assuming that the transmitter antennas and the receiver antennas are co-located (meaning that they are situated close together with respect to the distance to the target), so that the transmission angle and the receiver angle are the same θ_k. Let $y_m(n)$ denote the signal received by the mth receive antenna at instant n, and let

$$\mathbf{y}(n) = [y_1(n), y_2(n), \ldots, y_M(n)]^T, \text{ with } n = 1, \ \ldots, \ N.$$

The receiving steering vector is

$$\mathbf{b}(\theta_k) = [e^{j2\pi f_0 \tilde{t}_1(\theta_k)}, e^{j2\pi f_0 \tilde{t}_2(\theta_k)}, \ldots, e^{j2\pi f_0 \tilde{t}_M(\theta_k)}]^T,$$

where $\tilde{t}_m(\theta_k)$ is the time needed by the signal reflected by the target located at θ_k to arrive at the mth receive antenna. Then, the received data vector can be described by the equation [20]

$$\mathbf{y}(n) = \sum_{k=1}^{K} \beta_k \mathbf{b}^*(\theta_k)\mathbf{a}^H(\theta_k)\mathbf{x}(n) + \boldsymbol{\epsilon}(n), \text{ with } n = 1, \ \ldots, \ N, \tag{2.2}$$

where K is the number of targets that reflect the signals back to the radar receiver, β_k are complex amplitudes proportional to the radar cross sections (RCSs) of those targets, θ_k are the target location parameters, and $\boldsymbol{\epsilon}(n)$ denotes the interference-plus-noise term.

2.2 Statistical Properties for MIMO Transmission Waveform

MIMO radar transmission signal design problem is often associated with statistical properties possessed by the signal sequence, which should not only match an appropriate transmission covariance matrix, but also present good auto-correlation and cross-correlation properties [21].

Consider the transmitted signals from all the antennas within a period. The covariance matrix of $\mathbf{X}$ (2.1) is $\mathbf{R} = \mathbb{E}(\mathbf{X}\mathbf{X}^H)$. The "spatial spectrum" [17], which is also called the transmission beampattern, is the transmission power as a function of the angle θ. It is expressed as $P(\theta) = \mathbf{a}^H(\theta)\mathbf{R}\mathbf{a}(\theta)$.

Now, let us see the correlation properties of the waveforms [4]. The expression

$$r_{m_1 m_2}(\tau) = \sum_{t=1}^{N-\tau} x_{m_1}(t+\tau) x_{m_2}^*(t) = r_{m_2 m_1}(-\tau),$$
$$\text{with } 1 \le m_1 \le M\,, 1 \le m_2 \le M, \tau = 0, 1, 2, \ldots. \quad (2.3)$$

denotes the correlation between the m_1th and m_2th sequences at time lag τ. (M is the transmission antenna number.)

Different integers of m_1 and m_2 bring different interpretations of $r_{m_1 m_2}(\tau)$. If $m_1 = m_2$, $r_{mm}(\tau)$ is the auto-correlation of the mth antenna at time lag τ. If $m_1 \neq m_2$, $r_{m_1 m_2}(\tau)$ indicates the cross-correlation between the m_1 and m_2 antennas at time lag τ.

Good auto-correlation and cross-correlation properties of the transmitted waveforms are also often required in range compression applications. Good auto-correlation

means that a transmitted waveform is nearly uncorrelated with its own time-shifted versions, while good cross-correlation indicates that any one of the transmitted waveforms is nearly uncorrelated with other time-shifted transmitted waveforms. This kind of design ensures that matched filters at the receiver end can easily extract the signals backscattered from the range bin of interest while attenuating signals backscattered from other range bins [3]. Therefore, the values associated with $r_{m_1 m_2}(\tau)$ should be small enough for all τ when $m_1 \neq m_2$.

Using (2.3), we can represent the waveform correlation matrices for different time lags [3] as

$$\mathbf{R}_\tau = \begin{bmatrix} r_{11}(\tau) & r_{12}(\tau) & \dots & r_{1M}(\tau) \\ r_{21}(\tau) & r_{22}(\tau) & \dots & r_{2M}(\tau) \\ \vdots & \vdots & \ddots & \vdots \\ r_{M1}(\tau) & r_{M2}(\tau) & \dots & r_{MM}(\tau) \end{bmatrix}, \text{with } -N+1 \leq \tau \leq N-1. \tag{2.4}$$

It should be noticed that when $\tau = 0$, it is the covariance matrix of $\boldsymbol{x}$ mentioned above. When $\tau \neq 0$, the diagonal elements in $\mathbf{R}_\tau$ specify the auto-correlations of the antennas in the system, and the off-diagonal elements specify the cross-correlations of the antennas.

2.3 MIMO Radar Waveform Synthesis with Euclidean Distance (ED)

In this section, we will talk about the syntheses of MIMO radar waveform based on the previous discussed statistical properties. Both [3] and [4] propose Cyclic Algorithms

(CA) in dealing with this optimization problem. Reference [5] implements a quasi-Newton iterative algorithm to solve this problem.

Signal Design with Cyclic Algorithms

The main waveform design problem is to synthesize the discrete waveform with good correlation properties. Then the objective in [3] is formulated as

$$\varepsilon = \sum_{m=1}^{M} \sum_{\tau=-N+1,\tau\neq 0}^{N-1} |r_{mm}(\tau)|^2 + \sum_{m_1=1}^{M} \sum_{m_2=1,m_2\neq m_1}^{M} \sum_{\tau=-N+1}^{N-1} |r_{m_1m_2}(\tau)|^2 \ , \tag{2.5}$$

in which the first term is the auto-correlation of the signal sequence, and the second term is the cross-correlation. Given the waveform correlation matrices in (2.4), defining a shifting $N \times N$ matrix $\mathbf{J}_\tau$ as

$$\mathbf{J}_\tau = \begin{bmatrix} \overbrace{0\cdots 0}^{\tau \text{ zeros}} & 1 & & \mathbf{0} \\ & & \ddots & \\ & & & 1 \\ \mathbf{0} & & & \end{bmatrix} = \mathbf{J}_{-\tau}^T, \text{ with } 0 \leq \tau \leq N-1, \tag{2.6}$$

then the shifted transmitted signal of $\mathbf{X}$ in (2.1) can be written as

$$\mathbf{X}\mathbf{J}_\tau^T = \begin{bmatrix} x_1(\tau+1) & x_1(\tau+2) & \dots & x_1(N) & \\ x_2(\tau+1) & x_2(\tau+2) & \dots & x_2(N) & \\ \vdots & \vdots & \ddots & \vdots & \mathbf{0}_{M\times\tau} \\ x_M(\tau+1) & x_M(\tau+2) & \dots & x_M(N) & \end{bmatrix}.$$

Referring to the expression of (2.3), the correlation matrices (2.4) can be rewritten as the product of $\mathbf{X}\mathbf{J}_\tau^T$ and $\mathbf{X}^H$, which is

$$
\begin{aligned}
&\mathbf{X}\mathbf{J}_\tau^T\mathbf{X}^H \\
&= \begin{bmatrix} x_1(\tau+1) & x_1(\tau+2) & \dots & x_1(N) & \\ x_2(\tau+1) & x_2(\tau+2) & \dots & x_2(N) & \\ \vdots & \vdots & \ddots & \vdots & \mathbf{0}_{M\times\tau} \\ x_M(\tau+1) & x_M(\tau+2) & \dots & x_M(N) & \end{bmatrix} \begin{bmatrix} x_1^*(1) & x_2^*(1) & \dots & x_M^*(1) \\ x_1^*(2) & x_2^*(2) & \dots & x_M^*(2) \\ \vdots & \vdots & \ddots & \vdots \\ x_1^*(N) & x_2^*(N) & \dots & x_M^*(N) \end{bmatrix} \\
&= \begin{bmatrix} \cdots & x_1(\tau+1)x_{m_2}^*(1)+\cdots+x_1(N)x_{m_2}^*(N-\tau) & \cdots \\ \vdots & \vdots & \vdots \\ \cdots & x_{m_1}(\tau+1)x_{m_2}^*(1)+\cdots+x_{m_1}(N)x_{m_2}^*(N-\tau) & \cdots \\ & \cdots & \end{bmatrix} \\
&= \begin{bmatrix} \sum_{t=1}^{N-\tau} x_1(t+\tau)x_1^*(t) & \sum_{t=1}^{N-\tau} x_1(t+\tau)x_2^*(t) & \cdots \\ \vdots & \vdots & \vdots \\ & \sum_{t=1}^{N-\tau} x_{m_1}(t+\tau)x_{m_2}^*(t) & \\ & \cdots & \end{bmatrix} \\
&= \mathbf{R}_\tau = \mathbf{R}_{-\tau}^H.
\end{aligned}
$$

With this newly defined notation $\mathbf{R}_\tau = \mathbf{X}\mathbf{J}_\tau^T\mathbf{X}^H$, the expression in (2.5) can be rewritten as

$$\varepsilon = \|\mathbf{R}_0 - N\mathbf{I}_M\|^2 + 2\sum_{\tau=1}^{N-1}\|\mathbf{R}_\tau\|^2. \tag{2.7}$$

Using the notation that $\delta_\tau = \begin{cases} 0 & \tau \neq 0 \\ 1 & \tau = 0 \end{cases}$, we can express the design criterion as

$$\varepsilon = \sum_{\tau=-N+1}^{N-1} \|\mathbf{R}_\tau - N\mathbf{I}_M\delta_\tau\|^2. \tag{2.8}$$

Define $\mathbf{\Phi}(\omega_p) \triangleq \sum_{\tau=-N+1}^{N-1} \mathbf{R}_\tau e^{-j\omega_p\tau}$, in which $\omega_p = \frac{2\pi}{2N}p$, $p = 1, \ \ldots, \ 2N$. This is the cross-power spectral density matrix of the vector sequence $\mathbf{x}(\tau) = [x_1(\tau)\cdots x_M(\tau)]^T$. Then $\mathbf{\Phi}(\omega_p)$ can be written as the following form,

$$\mathbf{\Phi}(\omega_p) = \widetilde{\mathbf{y}}(\omega_p)\widetilde{\mathbf{y}}^H(\omega_p), \tag{2.9}$$

where

$$\widetilde{\mathbf{y}}(\omega_p) = \sum_{\tau=1}^{N} \mathbf{y}(\tau)e^{-j\omega_p\tau}, \ \mathbf{y}(\tau) = [x_1(\tau) \ x_2(\tau)\cdots x_M(\tau)]^T.$$

It follows from $\mathbf{\Phi}(\omega_p)$ and (2.9) that (2.8) can be written as

$$\begin{aligned} \varepsilon &= \frac{1}{2N}\sum_{p=1}^{2N} \|\mathbf{\Phi}(\omega_p) - N\mathbf{I}_M\|^2 \\ &= \frac{1}{2N}\sum_{p=1}^{2N} \|\widetilde{\mathbf{y}}(\omega_p)\widetilde{\mathbf{y}}^H(\omega_p) - N\mathbf{I}_M\|^2. \end{aligned} \tag{2.10}$$

Writing $\widetilde{\mathbf{y}}_p \triangleq \widetilde{\mathbf{y}}(\omega_p)$, and further simplifying Eq (2.10), we have

$$\begin{aligned}\varepsilon &= \frac{1}{2N}\sum_{p=1}^{2N}\mathrm{tr}[(\widetilde{\mathbf{y}}_p\widetilde{\mathbf{y}}_p^H - N\mathbf{I}_M)(\widetilde{\mathbf{y}}_p\widetilde{\mathbf{y}}_p^H - N\mathbf{I}_M)^H] \\ &= \frac{1}{2N}\sum_{p=1}^{2N}(\|\widetilde{\mathbf{y}}_p\|^4 - 2N\|\widetilde{\mathbf{y}}_p\|^2 + N^2M) \\ &= 2N\sum_{p=1}^{2N}\left(\left\|\frac{\widetilde{\mathbf{y}}_p}{\sqrt{2N}}\right\|^2 - \frac{1}{2}\right)^2 + N^2(M-1). \end{aligned} \tag{2.11}$$

From (2.11) it can be noticed that ε is lower bounded by $N^2(M-1)$ and therefore the correlations of the signal sequences cannot be made very small.

From the above discussion, the optimization problem could be considered in a simpler form as

$$\begin{aligned}&\min_{\mathbf{X},\{\boldsymbol{\alpha}_p\}_{p=1}^{2N}} \sum_{p=1}^{2N}\|\frac{\widetilde{\boldsymbol{y}}_p}{\sqrt{2N}} - \boldsymbol{\alpha}_p\|^2 \\ &\text{s.t.}\,|x_m(\tau)| = 1,\ m = 1,\ \ldots,\ M,\ n = 1,\ \ldots,\ N \\ &\qquad \|\boldsymbol{\alpha}_p\|^2 = \frac{1}{2},\ p = 1,\ \ldots,\ 2N\ (\boldsymbol{\alpha}_p \in \mathbb{C}^{M\times 1}).\end{aligned} \tag{2.12}$$

To solve this minimization problem, define

$$\begin{aligned}\mathbf{a}_p^H &= [e^{-j\omega_p}\ldots e^{-j2N\omega_p}], \\ \mathbf{A} &= \frac{1}{\sqrt{2N}}[\mathbf{a}_1\ldots\mathbf{a}_{2N}], \\ \widetilde{\mathbf{X}}^T &= [\mathbf{X}\ \mathbf{0}]_{M\times 2N}, \\ \mathbf{V} &= [\boldsymbol{\alpha}_1\ldots\boldsymbol{\alpha}_{2N}]^T,\end{aligned}$$

and then the objective function in (2.12) is observed to be

$$\|\mathbf{A}^H\widetilde{\mathbf{X}} - \mathbf{V}\|^2 = \|\widetilde{\mathbf{X}} - \mathbf{A}\mathbf{V}\|^2.$$

In [3] a Cyclic algorithm is proposed to solve this problem, which is summarized in Table 2.1.

Table 2.1: Cyclic Algorithm (CAN) [3]

Step 0:	Initialize $\mathbf{X}$ by a randomly generated $M \times N$ matrix.
Step 1:	Fix $\widetilde{\mathbf{X}}$ and compute $\mathbf{V}$.
Step 2:	Fix $\mathbf{V}$ and compute $\widetilde{\mathbf{X}}$.
Step 3:	Repeat Steps 1 and 2 until the pre-specified stop criterion is satisfied.

The result for the numerical examples of the signal sequence with $N = 40$ samples and $M = 3$ transmission antennas in [3] is compared with that of the cross entropy (CE) sequence in [22], which is shown in Fig. 2.1.

Here, we just give a general description for CE method used in [22]. The optimization problem is

$$\min_{\mathbf{P}} \Big\{ E_{\mathbf{P}} \Big\{ I_{\{E(\mathbf{X}) \leq e\}} \ln \frac{I_{\{E(\mathbf{X}) \leq m\}} f(\mathbf{X}, \hat{\mathbf{P}})}{f(\mathbf{X}, \mathbf{P})} \Big\} \Big\}.$$

This can be translated into the choice of an optimum parameter $\mathbf{P}$, which can be found by minimizing the CE between the two distributions $f(\mathbf{X}, \hat{\mathbf{P}})$ and $g^*(\mathbf{X})$. The original parameterized family of density is denoted as $f(\mathbf{X}, \hat{\mathbf{P}})$. The matrix of probability is $\mathbf{P}$, such that the element $\mathbf{P}(m, n, p)$ denotes the probability that the element $\mathbf{X}(m, n)$ has a phase p. A collection of indicator functions on $\mathbf{X}$ for

various threshold levels e is denoted as $I_{\{E(\mathbf{X})\leq e\}}$. The optimal $g^*(\mathbf{X}_i)$ is given as $\frac{I_{\{E(\mathbf{X}_i)\leq e\}} f(\mathbf{X}_i,\hat{\mathbf{P}})}{l}$, in which l is the probability that the performance function $E(\mathbf{X})$ is less than or equal to the threshold e.

Since $\hat{\mathbf{P}}$ is determined, the optimum $\mathbf{P}$ for the jth iteration is shown as

$$\mathbf{P}_i^{(j)} = \frac{\sum_{i=1}^{N} I_{\{E(\mathbf{X}_i^{(j)})\leq e\}} \mathbf{X}_i^{(j)}}{\sum_{i=1}^{N} I_{\{E(\mathbf{X}_i^{(j)})\leq e\}}}.$$

The CE procedure used in [22] is divided into two phases: generating N random samples of signal sequence and then updating the parameters.

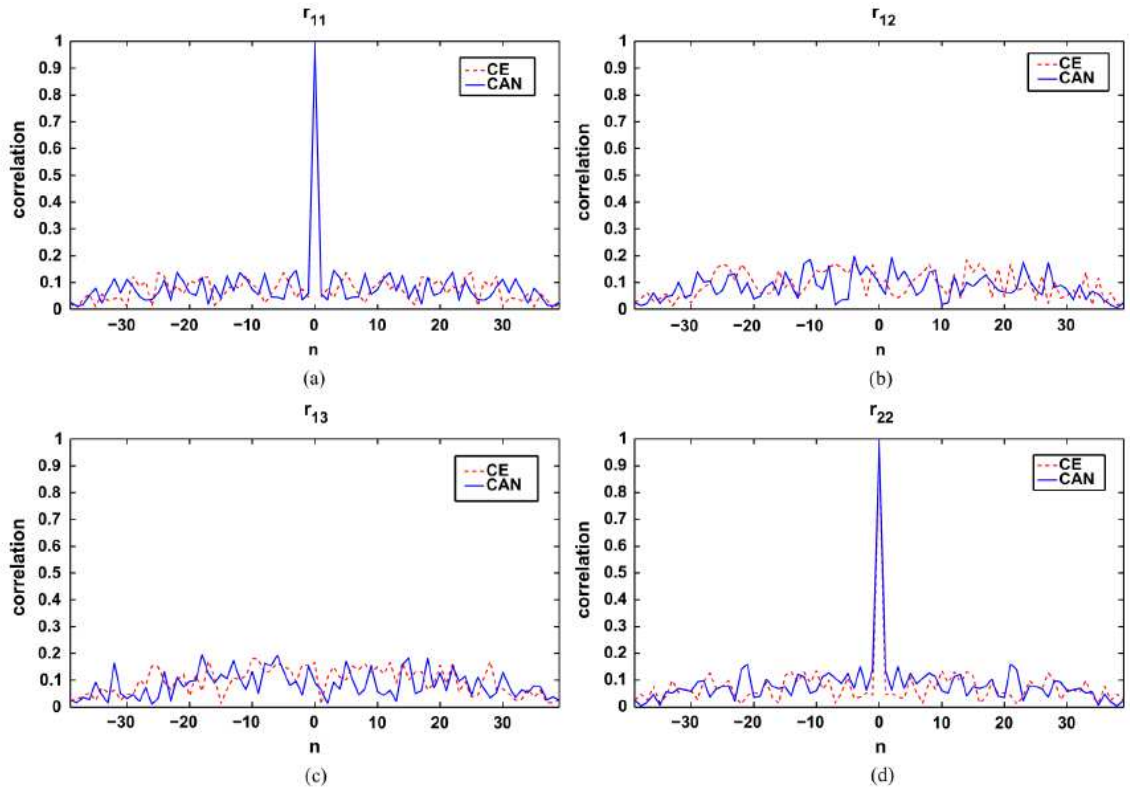

Figure 2.1: Correlations of the 3×40 CAN and CE Sequences [3]

Instead of considering the correlation properties of the whole length of the signal sequences, the work in [4] considers the waveform correlation properties within a certain lag interval $P-1 < N$ (N is length of the transmitted sequences). The reason is that in some radar applications like synthetic aperture radar imaging, the transmitted pulse is relatively long so that the signals backscattered from objects in the near and far range bins overlap significantly. In this case, only the waveform correlation properties in a certain lag interval are relevant to range resolution [3].

In this case, a proper minimization criterion is formed as

$$\widetilde{\varepsilon} = \|\mathbf{R}_0 - N\mathbf{I}_M\|^2 + 2\sum_{\tau=1}^{P-1}\|\mathbf{R}_\tau\|^2. \tag{2.13}$$

This optimization problem is solved directly in [4]. Unlike the method introduced from (2.8) to (2.12), the correlation matrix in [4] is given as $\widetilde{\mathbf{X}}\widetilde{\mathbf{X}}^H$, in which $\widetilde{\mathbf{X}}$ is the block-Toeplitz matrix

$$\widetilde{\mathbf{X}} = \overbrace{\begin{bmatrix} x_1(1) & \cdots & x_1(N) & & \mathbf{0} \\ \vdots & \ddots & & \ddots & \\ \mathbf{0} & & x_1(1) & \cdots & x_1(N) \\ & & \vdots & & \\ x_M(1) & \cdots & x_M(N) & & \mathbf{0} \\ \vdots & \ddots & & \ddots & \\ \mathbf{0} & & x_M(1) & \cdots & x_M(N) \end{bmatrix}}^{N+P-1}.$$

Note that $\widetilde{\mathbf{X}} \in \mathbb{C}^{MP\times(P+N-1)}$ and $MP < P+N-1$. Define $\widetilde{\mathbf{R}} = \mathbf{R}_0 \otimes \mathbf{I}_P$, and then

the optimization problem (2.13) can be written more compactly as

$$\min_{\mathbf{X}} \|\widetilde{\mathbf{X}}\widetilde{\mathbf{X}}^H - N\widetilde{\mathbf{R}}\|^2. \tag{2.14}$$

Introduce a semi-unitary matrix $\widetilde{\mathbf{U}}^H \in \mathbb{C}^{MP\times(P+N-1)}$ with $\widetilde{\mathbf{U}}^H\widetilde{\mathbf{U}} = \mathbf{I}_{MP}$, and then another mathematical formulation can be written as

$$\begin{aligned} &\min_{\mathbf{X},\widetilde{\mathbf{U}}} \|\widetilde{\mathbf{X}}^H - \sqrt{N}\widetilde{\mathbf{U}}\widetilde{\mathbf{R}}^{\frac{1}{2}}\|^2 \\ &\text{s.t. } \widetilde{\mathbf{U}}^H\widetilde{\mathbf{U}} = \mathbf{I}_{MP}. \end{aligned} \tag{2.15}$$

Let us see how (2.14) is transformed to (2.15). Suppose that the objective in (2.15) can reach 0, that is $\widetilde{\mathbf{X}}^H = \sqrt{N}\widetilde{\mathbf{U}}\widetilde{\mathbf{R}}^{\frac{1}{2}}$, then $\widetilde{\mathbf{X}}\widetilde{\mathbf{X}}^H = N\widetilde{\mathbf{R}}^{\frac{1}{2}H}\widetilde{\mathbf{U}}^H\widetilde{\mathbf{U}}\widetilde{\mathbf{R}}^{\frac{1}{2}} = N\widetilde{\mathbf{R}}$, which is the result for (2.14) when it equals to 0. However, (2.15) is non-convex due to the constraint $\widetilde{\mathbf{U}}^H\widetilde{\mathbf{U}} = \mathbf{I}_{MP}$. But it can also be solved by another CA proposed in [4], which is described briefly in Table 2.2. The work in [4] presents several numerical examples to demonstrate the effectiveness of this CA for signal synthesis. Fig. 2.2 shows the correlation levels of the CA synthesized waveforms under the constraints of PAR $= 1,$ PAR $\leq 1.1,$ PAR $\leq 2.$ (PAR stands for peak-to-average-power, whose definition is discussed in [4].)

Table 2.2: Cyclic Algorithm (CA) [4]

Step 0:	Set an initial value for $\widetilde{\mathbf{U}}$.
Step 1:	Fix $\widetilde{\mathbf{U}}$ and compute $\mathbf{X}$.
Step 2:	Fix $\mathbf{X}$ and determine $\widetilde{\mathbf{U}}$.
Step 3:	Repeat Steps 1 and 2 until a pre-specified stop criterion is satisfied.

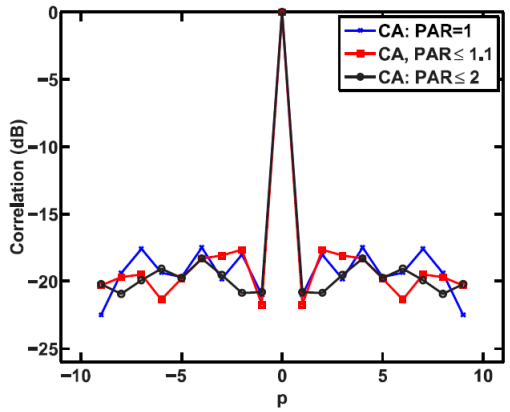

(a) $M = 10, N = 256, P = 1, \mathbf{R}_0 \neq \mathbf{I}_M$

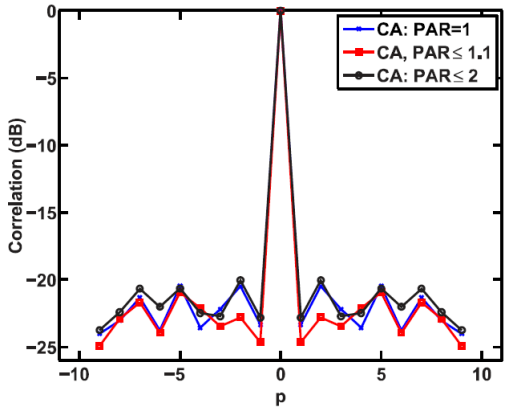

(b) $M = 10, N = 512, P = 1, \mathbf{R}_0 \neq \mathbf{I}_M$

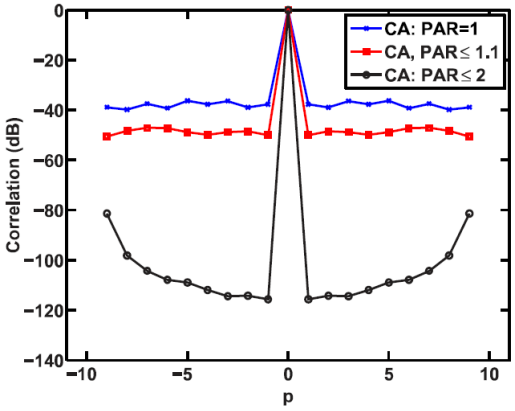

(c) $M = 10, N = 256, P = 10, \mathbf{R}_0 \neq \mathbf{I}_M$

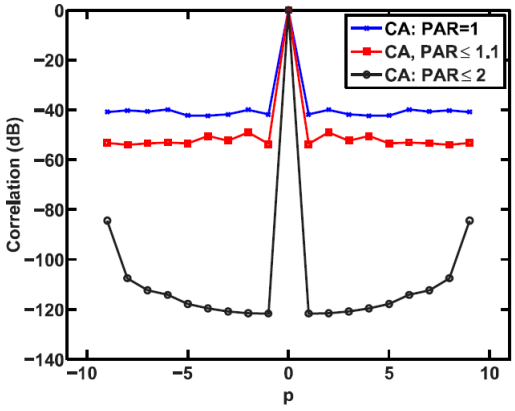

(d) $M = 10, N = 512, P = 10, \mathbf{R}_0 \neq \mathbf{I}_M$

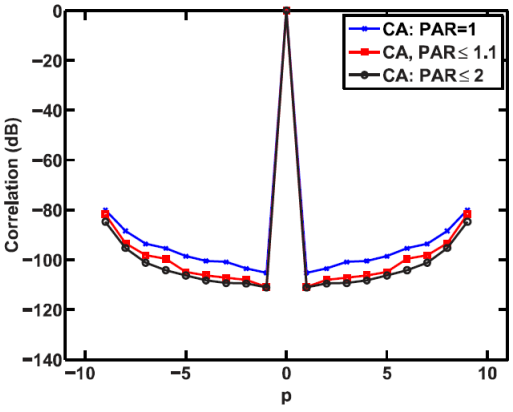

(e) $M = 10, N = 256, P = 10, \mathbf{R}_0 = \mathbf{I}_M$

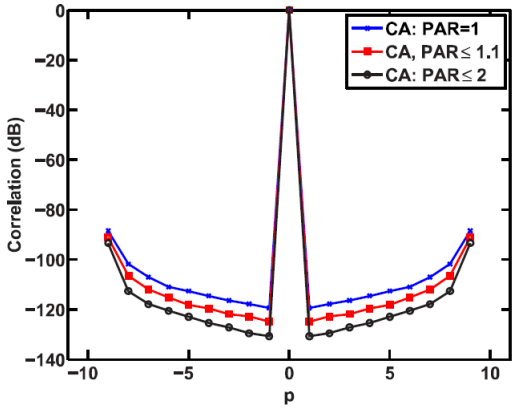

(f) $M = 10, N = 512, P = 10, \mathbf{R}_0 = \mathbf{I}_M$

Figure 2.2: Correlation Level for CA [4]

These two CAs are both effective in the signal design. Table 2.3 compares these two CA sequences with $M = 4, N = 256, P = 50$ in terms of the auto-correlation sidelobe peak, the cross-correlation peak and the ε defined in (2.11) and (2.13).

Table 2.3: Comparison between the Cyclic Algorithms (CAs) [3, 4]

	Auto-Correlation Sidelobe Peak	Cross-Correlation Peak	ε
CAN [3]:	-20.54	-18.19	0.91
CA [4]:	-21.08	-20.77	0.088

Signal Design with Quasi-Newton Algorithm

Similar to [4], the work in [5] optimizes the signal waveforms to meet the specification directly. But the work in [5] poses the problem as an unconstrained fourth-order minimization problem and uses a quasi-Newton iterative algorithm to solve it.

Consider that the MIMO radar transmission-reception array is uniform linear array and half wavelength inter-element spacing. With the same signal matrix (2.1) and a steering vector $\mathbf{a}_\theta = [1 \; e^{j\pi \sin\theta} \; \ldots \; e^{j\pi(M-1)\sin\theta}]$, in which $\mathbf{a}_\theta \in \mathbb{C}^{1\times M}$, and θ represents the spatial direction, the beam pattern describing the power distribution of the signals in the special domain is defined as

$$P(\theta) = \mathbf{a}_\theta^* \mathbf{X}^* \mathbf{X}^T \mathbf{a}_\theta^T. \tag{2.16}$$

By using the shifting matrix (2.6), the time delayed signal matrix is described as $\mathbf{J}_\tau^H \mathbf{X}^T$. Then the spatial auto-correlation and cross-correlation functions for $\mathbf{X}$

become

$$P_{\mathrm{ac}}(\tau,\theta_k)=\mathbf{a}_{\theta_k}^{*}\mathbf{X}^{*}\mathbf{J}_{\tau}\mathbf{X}^{T}\mathbf{a}_{\theta_k}^{T}, \tag{2.17}$$

$$P_{\mathrm{cc}}(\tau,\theta_i,\theta_j)=\mathbf{a}_{\theta_i}^{*}\mathbf{X}^{*}\mathbf{J}_{\tau}\mathbf{X}^{T}\mathbf{a}_{\theta_j}^{T}. \tag{2.18}$$

Because the beam pattern $P(\theta)$ in (2.16) describes the spatial power distribution of probing signals, the work in [5] suggests that a desired beam pattern $\mathbf{p}(\theta)$ can be specified to focus the signal power along the directions of interest. This can effectively reduce the impact of clutter and extend the detection distance. Moreover, minimizing the autocorrelation sidelobes aims to reduce the effects of clutter and lowering cross-correlation levels decreases the interference between signals from different directions. For these reasons, the work in [5] proposes the following optimization model:

$$\begin{aligned}&\min_{\mathbf{X},\alpha}\ \omega_b^2 e_b(\alpha,\mathbf{X})+\omega_{ac}^2 e_{ac}(\mathbf{X})+\omega_{cc}^2 e_{cc}(\mathbf{X})\\&\text{s.t. }\ |x_i(j)|=1, i=1,\ldots,M, j=1,\ldots,N\ ,\end{aligned} \tag{2.19}$$

where

$$\begin{aligned}e_b(\alpha,\mathbf{X})&=\sum_{\theta\in\Theta}|\alpha\mathbf{p}(\theta)-\mathbf{a}_{\theta}^{*}\mathbf{X}^{*}\mathbf{X}^{T}\mathbf{a}_{\theta}^{T}|^2,\\ e_{ac}(\mathbf{X})&=\sum_{\tau=1}^{N-1}\sum_{\theta_k\in\Theta}|\mathbf{a}_{\theta_k}^{*}\mathbf{X}^{*}\mathbf{J}_{\tau}\mathbf{X}^{T}\mathbf{a}_{\theta_k}^{T}|^2,\\ e_{cc}(\mathbf{X})&=\sum_{\tau=1}^{N-1}\sum_{\substack{\theta_i\neq\theta_j\\ \theta_i,\theta_j\in\Theta}}|\mathbf{a}_{\theta_i}^{*}\mathbf{X}^{*}\mathbf{J}_{\tau}\mathbf{X}^{T}\mathbf{a}_{\theta_j}^{T}|^2.\end{aligned}$$

In (2.19), α is an unknown scaling factor to be optimized. The weights ω_b, ω_{ac} and ω_{cc}

can make tradeoff of performances among matching desired beam pattern, suppressing auto-correlation and cross-correlation sidelobe levels. The parameter θ belongs to an angle set Θ representing the spacial direction.

Notice that the constant modulus constraints are equivalent to every entry of $\mathbf{X}$ (2.1) lying on the unit circle, $x_i(j) = e^{j\phi_i(j)}$. Using $\phi_i(j)$ as optimization variables and writing $\mathbf{X}$ as $\mathbf{X}(\boldsymbol{\phi})$ where $\boldsymbol{\phi}$ is an $M \times N$ matrix, the constant modulus constraints can be dropped and (2.19) is formulated as an unconstrained fourth order trigonometric polynomial minimization problem, that is $\min\limits_{\boldsymbol{\phi},\alpha} f(\alpha, \boldsymbol{\phi})$, where

$$f(\alpha, \boldsymbol{\phi}) = \omega_b^2 e_b(\alpha, \mathbf{X}(\boldsymbol{\phi})) + \omega_{ac}^2 e_{ac}(\mathbf{X}(\boldsymbol{\phi})) + \omega_{cc}^2 e_{cc}(\mathbf{X}(\boldsymbol{\phi})). \tag{2.20}$$

This unconstrained minimization model can be solved, approximately but effectively, using a quasi Newton algorithm, for example, L-BFGS (Limited-Memory Broyden-Fletcher-Goldfarb and Shannon algorithm, refer to [23]). A detailed description of this iterative algorithm is given in [5], in which the evaluation of $f(\alpha, \boldsymbol{\phi})$ and $\nabla f(\alpha, \boldsymbol{\phi})$ dominates the computational cost of each L-BFGS iteration. The significance in [5]'s work is to transform this original minimization problem into a new form that could be solved by L-BFGS efficiently, whose new expression is shown as follows,

$$\begin{aligned} f(\alpha, \boldsymbol{\phi}) =& \mathbf{v}(\alpha, \boldsymbol{\phi})^H \mathbf{Q} \mathbf{v}(\alpha, \boldsymbol{\phi}) + \\ & \omega_{ac} \sum_{\theta_k \in \Theta} \|\mathbf{c}_{\theta_k}^*(\boldsymbol{\phi}) \otimes \bar{\mathbf{c}}_{\theta_k}(\boldsymbol{\phi})\|^2 + \omega_{cc} \sum_{\substack{\theta_i \neq \theta_j \\ \theta_i, \theta_j \in \Theta}} \|\mathbf{c}_{\theta_i}^*(\boldsymbol{\phi}) \otimes \bar{\mathbf{c}}_{\theta_j}(\boldsymbol{\phi})\|^2, \end{aligned} \tag{2.21}$$

where

$\otimes$ is the convolution operator,

$$\mathbf{v}(\alpha, \boldsymbol{\phi}) = \begin{bmatrix} \alpha \\ \mathrm{vec}(\mathbf{X}^T(\boldsymbol{\phi}))^H \mathrm{vec}(\mathbf{X}^T(\boldsymbol{\phi})) \end{bmatrix},$$

$$\mathbf{Q} = \omega_b^2 \begin{bmatrix} \sum_{\theta\in\Theta} \mathbf{p}^2(\theta) & -\left[\sum_{\theta\in\Theta} \mathbf{p}(\theta)\mathrm{vec}(\mathbf{a}_\theta^T \mathbf{a}_\theta^*)\right]^H \\ -\sum_{\theta\in\Theta} \mathbf{p}(\theta)\mathrm{vec}(\mathbf{a}_\theta^T \mathbf{a}_\theta^*) & \sum_{\theta\in\Theta} \mathrm{vec}(\mathbf{a}_\theta^T \mathbf{a}_\theta^*)\mathrm{vec}^H(\mathbf{a}_\theta^T \mathbf{a}_\theta^*) \end{bmatrix},$$

$$\mathbf{c}_{\theta_k}(\boldsymbol{\phi}) = \mathbf{X}^T(\boldsymbol{\phi})\mathbf{a}_{\theta_k}^T.$$

Table 2.4 shows a rough comparison of the complexity to compute $f(\alpha, \boldsymbol{\phi})$ and $\nabla f(\alpha, \boldsymbol{\phi})$ using original expression (2.20) and new expression (2.21), in which the antenna number, waveform length, spacial direction number and delay are denoted by $M,\ N,\ K,\ d$. Simulation results are shown in Fig.2.3.

Table 2.4: Comparison of the Complexity to Compute f and ∇f [5]

	Original Expression (2.20)	New Expression (2.21)
$f(\alpha, \boldsymbol{\phi})$:	$\mathcal{O}(\lvert\Theta\rvert N + K^2 dN)$	$\mathcal{O}(M^4 + 6K^2 N \log_2 2N)$
$\nabla f(\alpha, \boldsymbol{\phi})$:	$\mathcal{O}(3\lvert\Theta\rvert NM + 2K^2 dNM)$	$\mathcal{O}(2NM^2 + K^2 dNM)$

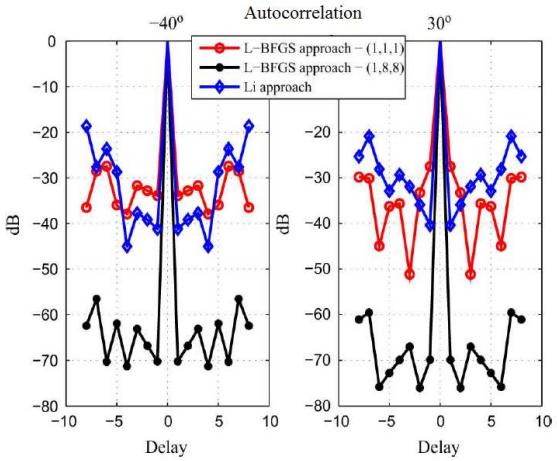

(a) $M = 8,\ N = 32,\ \text{delay} = 8$

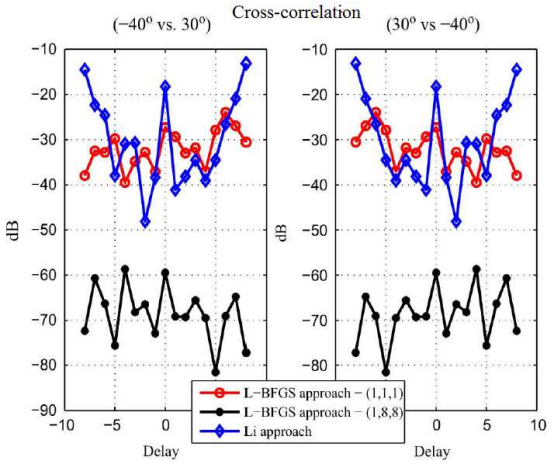

(b) $M = 8,\ N = 32,\ \text{delay} = 8$

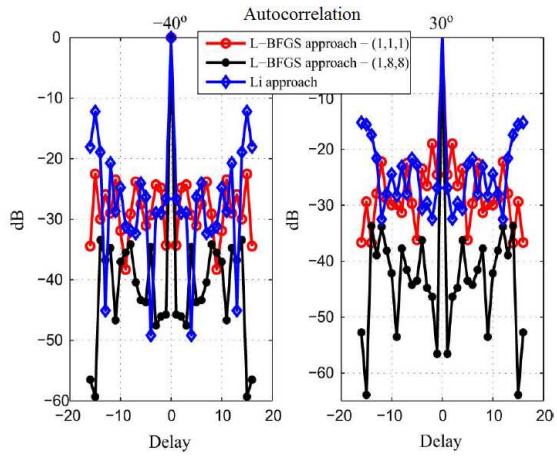

(c) $M = 8,\ N = 32,\ \text{delay} = 16$

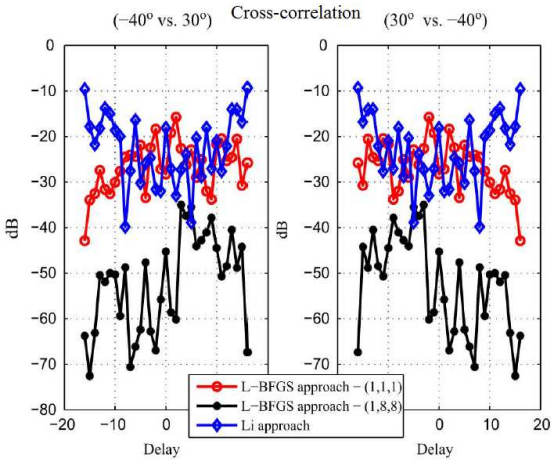

(d) $M = 8,\ N = 32,\ \text{delay} = 16$

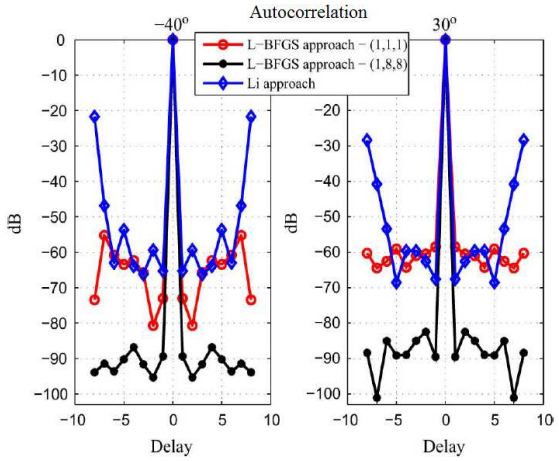

(e) $M = 8,\ N = 128,\ \text{delay} = 8$

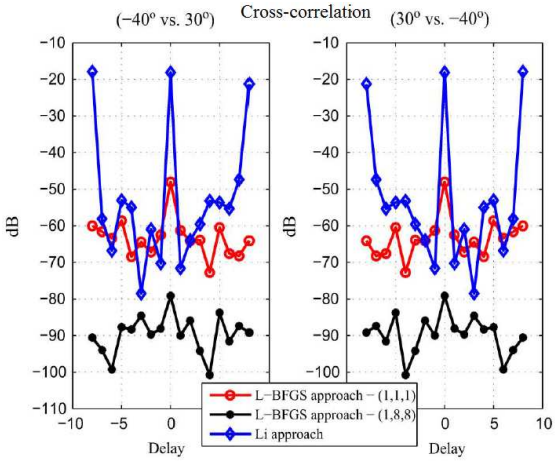

(f) $M = 8,\ N = 128,\ \text{delay} = 8$

Figure 2.3: Correlation Characteristics by L-BFGS [5]

Chapter 3

Waveform Synthesis with Riemannian Distance

As we have mentioned before, there is an extensive literature about the MIMO radar waveform design [5, 2, 16, 14, 19, 17, 24, 13, 25] focusing on the optimization of covariance matrix $\mathbf{R}$. In these former works, the Euclidean Distance (ED) is used as a metric to measure the difference between two positive semi-definite (PSD) matrices. In this chapter, we will introduce a new metric, Riemannian Distance (RD), as a measurement of the difference. Due to the special structure of the PSD matrix, it has been proved in [18] that RD is more precise for calculating the distance between two PSD matrices. With the use of this measurement for the covariance matrix, we then propose a method of directly designing the signals by optimizing a given performance measure with the usage of RD metric.

3.1 Introduction to Riemannian Distance (RD)

In signal synthesis, the Frobenius Norm (FN) $\|\cdot\|$ is usually used to evaluate the difference $\mathbf{\Delta}$ between two covariance matrices, $\mathbf{R}$ and $\mathbf{R}_d$, such that

$$\begin{aligned} \mathbf{\Delta} &= \mathbf{R} - \mathbf{R}_d \ , \\ \|\mathbf{\Delta}\|_F &= \sqrt{\mathrm{tr}(\mathbf{\Delta}^H \mathbf{\Delta})} \ . \end{aligned} \tag{3.1}$$

This comes from the Frobenius inner product of $\langle \mathbf{\Delta}, \mathbf{\Delta} \rangle$, so it can be considered as the ED between $\mathbf{R}$ and $\mathbf{R}_d$. While this Euclidean metric is the most commonly used distance measurement in signal processing, it may not be the most appropriate one for the covariance matrix of the transmitted signals. In our problem, the covariance matrix of the transmitted signals has the special structure, that is, Hermitian symmetric and positive semi-definite. As discussed in [18], these properties describe a hyper-surface, called a manifold $\mathcal{M}$, in the signal space on which the points of PSD matrices are located. Therefore, we can say that our covariance matrix describes a manifold, a Riemannian manifold, to be more specific. The definition of RD has been given in [18], in which three kinds of RD are also derived. Theorem 1 defines the first RD between two points $\mathbf{P}_1, \mathbf{P}_2 \in \mathcal{M}$, and Theorem 2 defines the second RD.

Theorem 1. *For $\mathbf{P}_1, \mathbf{P}_2 \in \mathcal{M}$, a RD between $\mathbf{P}_1$ and $\mathbf{P}_2$ is given by*

$$d_{R_1}(\mathbf{P}_1, \mathbf{P}_2) = \sqrt{\mathrm{tr}\mathbf{P}_1 + \mathrm{tr}\mathbf{P}_2 - 2\mathrm{tr}\left[\left(\mathbf{P}_1^{\frac{1}{2}} \mathbf{P}_2 \mathbf{P}_1^{\frac{1}{2}}\right)^{\frac{1}{2}}\right]} \tag{3.2}$$

with the mapping π: $\tilde{\mathcal{H}} \to \mathcal{M}$ be chosen to be $\mathbf{P} = \tilde{\mathbf{P}}\tilde{\mathbf{P}}^H$.

Theorem 2. *With the mapping π: $\tilde{\mathcal{H}} \to \mathcal{M}$ be given by $\mathbf{P} = \tilde{\mathbf{P}}^2$, the RD between $\mathbf{P}_1$*

and $\mathbf{P}_2$ *on* $\mathcal{M}$ *is*

$$d_{R_2}(\mathbf{P}_1, \mathbf{P}_2) = \sqrt{\text{tr}\mathbf{P}_1 + \text{tr}\mathbf{P}_2 - 2\text{tr}\left[\mathbf{P}_1^{\frac{1}{2}}\mathbf{P}_2^{\frac{1}{2}}\right]}. \tag{3.3}$$

If the product of $\mathbf{P}_1^{\frac{1}{2}}\mathbf{P}_2^{\frac{1}{2}}$ is a Hermitian matrix, i.e., they are commutative, then $\mathbf{U}_1 = \mathbf{U}_2$. Then we will have $d_{R_1} = d_{R_2}$.

The Euclidean distance shown in (3.1) measuring the straight line distance between the two points may be less appropriate than Riemannian distance. This concept is akin to finding the distance between two cities on earth. As mentioned before, $\mathbf{R}$ and $\mathbf{R}_d$ are positive definite Hermitian matrices forming a manifold in the signal space. Then the distance between these two matrices should be measured along the shortest path on the manifold between the points. Thus, we should use the RD to measure the difference between $\mathbf{R}$ and $\mathbf{R}_d$ on the covariance matrix manifold. In particular, since the second RD is more approachable, d_{R_2} will be employed in the signal synthesis problem discussed here.

3.2 Transmission Signal Sequence Design with Riemannian Distance (RD)

In this section, we develop the approach for signal synthesis using RD as a measure of estimation error between covariance matrices. Let us consider the scenario of a MIMO radar equipped with M transmission antennas. Let the transmitted signal $x_m(t)$ from the mth antenna be made up of a linear combination of orthonormal basis

functions such that

$$x_m(t) = \sum_{i=1}^{K} \alpha_{mi} s_i(t), \text{ with } 1 \leq t \leq N,\ 1 \leq m \leq M,$$

where N denotes the number of samples in each sampled waveform. And the coefficient vector associated with the mth antenna signal is

$$\boldsymbol{\alpha}_m = [\alpha_{m1}, \alpha_{m2}, \ldots, \alpha_{mK}] \in \mathbb{C}^{1\times K}.$$

In the above expression, $\{s_i(t)\}_{i=1}^{K}$ is the orthonormal basis, which means

$$\langle s_i(t), s_j(t) \rangle = \sum_t s_i(t) s_j^*(t) = \begin{cases} 1, & i = j \\ 0, & i \neq j \end{cases}.$$

The total number of orthonormal bases used in the signal synthesis problem is K (different from the K defined in Chapter 2), and $\langle \cdot \rangle$ is the inner product of two complex numbers.

Let the row vectors of $\mathbf{X} \in \mathbb{C}^{M\times N}$ be the transmitted waveforms from the antennas, and then the sampled version of the transmitted waveform can be given as

$$\mathbf{X} = \begin{bmatrix} x_1(1) & x_1(2) & \ldots & x_1(N) \\ x_2(1) & x_2(2) & \ldots & x_2(N) \\ \vdots & \vdots & \ddots & \vdots \\ x_M(1) & x_M(2) & \ldots & x_M(N) \end{bmatrix} \tag{3.4}$$

If we represent the sampled orthonormal bases by a matrix $\mathbf{S} \in \mathbb{C}^{K\times N}$, such that

$$\mathbf{S} = \begin{bmatrix} s_1(1) & s_1(2) & \dots & s_1(N) \\ s_2(1) & s_2(2) & \dots & s_2(N) \\ \vdots & \vdots & \ddots & \vdots \\ s_K(1) & s_K(2) & \dots & s_K(N) \end{bmatrix}, \tag{3.5}$$

and the coefficient matrix as $\mathbf{A} \in \mathbb{C}^{M\times K}$,

$$\mathbf{A} = \begin{bmatrix} \alpha_{11} & \alpha_{12} & \dots & \alpha_{1K} \\ \alpha_{21} & \alpha_{22} & \dots & \alpha_{2K} \\ \vdots & \vdots & \ddots & \vdots \\ \alpha_{M1} & \alpha_{M2} & \dots & \alpha_{MK} \end{bmatrix}, \tag{3.6}$$

then the transmitted signal can be rewritten as $\mathbf{X} = \mathbf{AS}$ in brief.

Since there are several methods to generate the orthonormal bases, $\mathbf{A}$ will be the only unknown variable focused on in our work.

Let $\mathbf{R}_0 = \mathbf{X}\mathbf{X}^H$ be the covariance matrix of the transmitted waveforms. Since the orthonormal bases are represented in discrete format, then $\mathbf{S}\mathbf{S}^H \approx \mathbf{I}_K$ and we will have

$$\mathbf{R}_0 = \mathbf{X}\mathbf{X}^H = \mathbf{A}\mathbf{S}\mathbf{S}^H\mathbf{A}^H \approx \mathbf{A}\mathbf{A}^H, \tag{3.7}$$

and $\mathbf{R}_0 \in \mathbb{R}^{M\times M}$, which is Hermitian and PSD matrix. Then the mathematical formulation of the problem of synthesizing the signal matrix $\mathbf{X}$ in terms of parameter matrix $\mathbf{A}$ using RD to match a desired covariance matrix $\mathbf{R}_d$ is as follows,

$$\min_{\mathbf{A}} \left\| \mathbf{A}\mathbf{A}^H - \mathbf{R}_d \right\|_R^2, \tag{3.8}$$

in which $\|\cdot\|_R$ represents the RD used in the measure of the difference between the positive definite Hermitian matrices.

As we mentioned in the previous chapter, in many real applications such as the matched filter reception, the good correlation properties possessed by waveforms are important requirements. Therefore, we also consider the auto-correlation and cross-correlation properties in the signal synthesis problem.

Let

$$r_{m_1 m_2}(\tau) = \sum_t x_{m_1}(t+\tau) x_{m_2}^*(t) = r_{m_2 m_1}^*(-\tau), \tag{3.9}$$
$$\text{with } 1 \le m_1 \le M\,, 1 \le m_2 \le M, \tau = 1, 2, \ldots, N-1.$$

Then the correlation matrix of the transmitted signals could be represented by

$$\mathbf{R}_\tau = \begin{bmatrix} r_{11}(\tau) & r_{12}(\tau) & \ldots & r_{1M}(\tau) \\ r_{21}(\tau) & r_{22}(\tau) & \ldots & r_{2M}(\tau) \\ \vdots & \vdots & \ddots & \vdots \\ r_{M1}(\tau) & r_{M2}(\tau) & \ldots & r_{MM}(\tau) \end{bmatrix}. \tag{3.10}$$

Now, we would like to express the correlation matrix $\mathbf{R}_\tau$ in terms of the parameter matrix $\mathbf{A}$ and the orthonormal basis matrix $\mathbf{S}$.

Because

$$x_{m_1}(t+\tau) = \sum_{i=1}^{K} \alpha_{m_1 i} s_i(t+\tau) \tag{3.11}$$
$$x_{m_2}(t) = \sum_{j=1}^{K} \alpha_{m_2 j} s_j(t) \ ,$$

then substituting these two expressions into (3.9), we get

$$\begin{aligned} r_{m_1 m_2}(\tau) &= \sum_{i=1}^{K}\sum_{j=1}^{K} \int_t \alpha_{m_1 i} s_i(t+\tau) \alpha^*_{m_2 j} s^*_j(t) dt \\ &= \sum_{i=1}^{K}\sum_{j=1}^{K} \alpha_{m_1 i} \alpha^*_{m_2 j} \int_t s_i(t+\tau) s^*_j(t) dt. \end{aligned} \tag{3.12}$$

Defining $\varphi_{ij}(\tau) = \int_t s_i(t+\tau) s^*_j(t) dt$, we get

$$r_{m_1 m_2}(\tau) = \sum_{i=1}^{K}\sum_{j=1}^{K} \alpha_{m_1 i} \alpha^*_{m_2 j} \varphi_{ij}(\tau), \text{ with } 1 \le m_1 \le M \, , 1 \le m_2 \le M.$$

Therefore, $\mathbf{R}_\tau$ could be formulated as

$$\mathbf{R}_\tau = \mathbf{A} \mathbf{\Phi}^T(\tau) \mathbf{A}^H, \tag{3.13}$$

in which

$$\mathbf{\Phi}(\tau) = \begin{bmatrix} \varphi_{11}(\tau) & \varphi_{21}(\tau) & \dots & r_{K1}(\tau) \\ \varphi_{12}(\tau) & \varphi_{22}(\tau) & \dots & \varphi_{K2}(\tau) \\ \vdots & \vdots & \ddots & \vdots \\ \varphi_{1K}(\tau) & \varphi_{2K}(\tau) & \dots & \varphi_{KK}(\tau) \end{bmatrix}. \tag{3.14}$$

To ensure the good auto-correlation and cross-correlation properties of transmitted signal $\mathbf{X}$, we need to guarantee the values of $\mathbf{R}_\tau$ at different lag τ to be small, such that

$$\left\|\mathbf{A}\mathbf{\Phi}^T(\tau)\mathbf{A}^H\right\|^2 \leq \varepsilon_\tau, \; \varepsilon_\tau \text{ is a small value.}$$

Consequently, a mathematical formulation of the problem of the signal synthesis using RD with time correlation considerations can be written as follows,

$$\begin{aligned} &\min_{\mathbf{A}} \left\|\mathbf{A}\mathbf{A}^H - \mathbf{R}_d\right\|_R^2 \\ &\text{s.t.} \left\|\mathbf{A}\mathbf{\Phi}^T(\tau)\mathbf{A}^H\right\|^2 \leq \varepsilon_\tau, \text{with } \tau \neq 0. \end{aligned} \tag{3.15}$$

3.3 Convex Design Problem

In this part, we would like to consider how to solve the optimization model (3.15).

First of all, let us transform the objective function in (3.15) into a mathematical form which could be applied in the convex optimization. In reality, the antenna number should not be too big because it would be costly to deploy a large antenna system. Therefore, in our problem, we consider the case of $K > M$, which means that the number of orthonormal basis is larger than that of antennas.

Considering the mapping condition in *Theorem 2*, such that $\mathbf{P}_1 = \mathbf{P}_1^{\frac{1}{2}}\mathbf{P}_1^{\frac{1}{2}}$ and $\mathbf{P}_2 = \mathbf{P}_2^{\frac{1}{2}}\mathbf{P}_2^{\frac{1}{2}}$, the expression for the second version of RD could be reformed as

$$\begin{aligned} d^2_{R_2}(\mathbf{P}_1, \mathbf{P}_2) &= \mathrm{tr}\mathbf{P}_1 + \mathrm{tr}\mathbf{P}_2 - 2\mathrm{tr}\left[\mathbf{P}_1^{\frac{1}{2}}\mathbf{P}_2^{\frac{1}{2}}\right] \\ &= \mathrm{tr}\left(\mathbf{P}_1^{\frac{1}{2}}\mathbf{P}_1^{\frac{1}{2}} + \mathbf{P}_2^{\frac{1}{2}}\mathbf{P}_2^{\frac{1}{2}} - 2\mathbf{P}_1^{\frac{1}{2}}\mathbf{P}_2^{\frac{1}{2}}\right) \\ &= \mathrm{tr}\left[\left(\mathbf{P}_1^{\frac{1}{2}} - \mathbf{P}_2^{\frac{1}{2}}\right)^H\left(\mathbf{P}_1^{\frac{1}{2}} - \mathbf{P}_2^{\frac{1}{2}}\right)\right] \\ &= \left\|\mathbf{P}_1^{\frac{1}{2}} - \mathbf{P}_2^{\frac{1}{2}}\right\|_2^2. \end{aligned}$$

Then the objective function of our problem by using RD could be reformulated as

$$d^2_{R_2}(\mathbf{A}\mathbf{A}^H, \quad \mathbf{R}_d) = \left\|(\mathbf{A}\mathbf{A}^H)^{\frac{1}{2}} - \mathbf{R}_d^{\frac{1}{2}}\right\|_2^2. \tag{3.16}$$

How can we calculate the square root of $\mathbf{A}\mathbf{A}^H$? First of all, let us perform the SVD on $\mathbf{A}$, such that

$$\begin{aligned} \mathbf{A} = \mathbf{V}\mathbf{\Sigma}\mathbf{U}^H &= \mathbf{V}\begin{bmatrix} \tilde{\mathbf{\Sigma}}_{M\times M} & \mathbf{0}_{M\times(K-M)} \end{bmatrix}\begin{bmatrix} \tilde{\mathbf{U}}^H \\ \tilde{\mathbf{U}}_0^H \end{bmatrix} \\ &= \begin{bmatrix} \mathbf{V}\tilde{\mathbf{\Sigma}} & \mathbf{0} \end{bmatrix}\begin{bmatrix} \tilde{\mathbf{U}}^H \\ \mathbf{U}_0^H \end{bmatrix} = \mathbf{V}\tilde{\mathbf{\Sigma}}\tilde{\mathbf{U}}^H, \end{aligned}$$

in which $\tilde{\mathbf{U}}^{\mathbf{H}} \in \mathbb{C}^{M\times K}$, $\mathbf{U}_0^H \in \mathbb{C}^{(K-M)\times K}$, $\mathbf{V} \in \mathbb{C}^{M\times M}$, $\tilde{\mathbf{\Sigma}} \in \mathbb{C}^{M\times M}$, and $\tilde{\mathbf{U}}^H\tilde{\mathbf{U}} = \mathbf{I}_M$.

Then, we can observe that

$$\begin{aligned}\mathbf{A}\mathbf{A}^H &= \mathbf{V}\tilde{\mathbf{\Sigma}}\tilde{\mathbf{U}}^H\tilde{\mathbf{U}}\tilde{\mathbf{\Sigma}}^H\mathbf{V}^H \\ &= \mathbf{V}\tilde{\mathbf{\Sigma}}\mathbf{I_M}\tilde{\mathbf{\Sigma}}^H\mathbf{V}^H \\ &= \mathbf{V}\tilde{\mathbf{\Sigma}}\tilde{\mathbf{\Sigma}}^H\mathbf{V}^H\end{aligned}$$

with $\mathbf{V}\tilde{\mathbf{\Sigma}} \in \mathbb{C}^{M\times M}$. Since $\mathbf{V}$ is a unitary matrix and $\tilde{\mathbf{\Sigma}}$ is a real diagonal matrix, we can see that the eigendecomposition of $\mathbf{A}\mathbf{A}^H$ is $\mathbf{V}(\tilde{\mathbf{\Sigma}}\tilde{\mathbf{\Sigma}}^H)\mathbf{V}^H$. Finally, we have

$$\begin{aligned}(\mathbf{A}\mathbf{A}^H)^{\frac{1}{2}} &= \mathbf{V}(\tilde{\mathbf{\Sigma}}\tilde{\mathbf{\Sigma}}^H)^{\frac{1}{2}}\mathbf{V}^H \\ &= \mathbf{V}\tilde{\mathbf{\Sigma}}\mathbf{V}^H. \end{aligned} \tag{3.17}$$

Moreover, we can also observe

$$\mathbf{A}\tilde{\mathbf{U}} = \mathbf{V}\tilde{\mathbf{\Sigma}}\tilde{\mathbf{U}}^H\tilde{\mathbf{U}} = \mathbf{V}\tilde{\mathbf{\Sigma}}\mathbf{I_M} = \mathbf{V}\tilde{\mathbf{\Sigma}}. \tag{3.18}$$

Finally, the result used in this problem for $(\mathbf{A}\mathbf{A}^H)^{\frac{1}{2}}$ is

$$(\mathbf{A}\mathbf{A}^H)^{\frac{1}{2}} = \mathbf{A}\tilde{\mathbf{U}}\mathbf{V}^H, \text{ with } \tilde{\mathbf{U}} \in \mathbb{C}^{K\times M} \text{ and } \mathbf{V}^H \in \mathbb{C}^{M\times M}. \tag{3.19}$$

By taking (3.19) into (3.16), the expression for the objective function is rewritten as

$$d^2_{R_2}(\mathbf{A}\mathbf{A}^H, \quad \mathbf{R}_d) = \left\|\mathbf{A}\tilde{\mathbf{U}}\mathbf{V}^H - \mathbf{R}_d^{\frac{1}{2}}\right\|_2^2. \tag{3.20}$$

Suppose that $\tilde{\mathbf{U}}$, $\mathbf{V}^H$ and $\mathbf{R}_d$ are all known, and then (3.20) will be a quadratic

form in terms of $\mathbf{A}$.

The argument $\left\|\mathbf{A}\mathbf{\Phi}^T(\tau)\mathbf{A}^H\right\|^2$ in the constraint of the problem (3.15) is not quadratic in $\mathbf{A}$. But if the last item $\mathbf{A}$ in $\left\|\mathbf{A}\mathbf{\Phi}^T(\tau)\mathbf{A}^H\right\|^2$ is known, then the expression $\left\|\mathbf{A}\mathbf{\Phi}^T(\tau)\mathbf{A}^H\right\|^2$ turns out to be in a quadratic form in terms of the first item $\mathbf{A}$, instead of a quartic form (i.e., the fourth order). In this sense, we apply the results of $\tilde{\mathbf{U}},\ \mathbf{V}^H$ and $\mathbf{A}$ from the previous iteration to substitute the item $\tilde{\mathbf{U}},\ \mathbf{V}^H$ in the objective function as well as the last item $\mathbf{A}$ in the constraint function in the current iteration.

If $\tilde{\mathbf{U}}_{n-1}, \mathbf{V}_{n-1}^H$ and $\mathbf{A}_{n-1}$ denote the results from the previous iteration, then the problem can be approximated as

$$\begin{aligned} &\min_{\mathbf{A}} \left\|\mathbf{A}\tilde{\mathbf{U}}_{n-1}\mathbf{V}_{n-1}^H - \mathbf{R}_d^{\frac{1}{2}}\right\|_2^2 \\ &\text{s.t.} \left\|\mathbf{A}\mathbf{\Phi}^T(\tau)\mathbf{A}_{n-1}^H\right\|^2 \leq \varepsilon_\tau,\ \tau = 1\ldots. \end{aligned} \tag{3.21}$$

The outline of this algorithm is given in Table 3.1, in which the value for $\mathbf{A}$ in our problem is initialized as the first M row vectors from a K-by-K matrix containing pseudorandom values drawn from the standard normal distribution.

Table 3.1: Iterative Algorithm

Step 0:	Set an initial value for $\mathbf{A}$, do SVD on $\mathbf{A}$ to get $\tilde{\mathbf{U}}$ and $\mathbf{V}$.
Repeat	
Step 1:	Fix $\widetilde{\mathbf{U}}_{n-1}$ and $\mathbf{V}_{n-1}$ in the objective, as well as one $\mathbf{A}_{n-1}$ in the constraint.
Step 2:	Compute $\mathbf{A}_n$.
Step 3:	Do SVD on $\mathbf{A}_n$ to get $\tilde{\mathbf{U}}_n$ and $\mathbf{V}_n$.

As we mentioned previously, if the product of $\mathbf{P}_1^{\frac{1}{2}}\mathbf{P}_2^{\frac{1}{2}}$ in d_{R_1} is a Hermitian matrix, i.e., they are commutative, d_{R_1} is equivalent to d_{R_2}. If $\mathbf{R}_d$ is chosen as an M-by-M identity matrix in our problem, we will have $d_{R_2} = d_{R_1}$.

Similarly, if the objective function in the problem (3.15) is measured by Frobenius Norm (FN), such that

$$d_E^2 = \left\|\mathbf{A}\mathbf{A}^H - \mathbf{R}_d\right\|_2^2, \tag{3.22}$$

then the corresponding optimization problem will be formulated as

$$\begin{aligned} &\min_{\mathbf{A}} \left\|\mathbf{A}\mathbf{A}_{n-1}^H - \mathbf{R}_d\right\|_2^2 \\ &\text{s.t.} \left\|\mathbf{A}\mathbf{\Phi}^T(\tau)\mathbf{A}_{n-1}^H\right\|^2 \leq \varepsilon_\tau,\ \tau = 1\ldots. \end{aligned} \tag{3.23}$$

For Riemannian Distance we have

$$\begin{aligned} d_{R_2}^2 &= \left\|\mathbf{A}\tilde{\mathbf{U}}\mathbf{V}^H - \mathbf{R}_d^{\frac{1}{2}}\right\|_2^2 \\ &= \mathrm{tr}\left[\left(\mathbf{A}\tilde{\mathbf{U}}\mathbf{V}^H - \mathbf{R}_d^{\frac{1}{2}}\right)\left(\mathbf{A}\tilde{\mathbf{U}}\mathbf{V}^H - \mathbf{R}_d^{\frac{1}{2}}\right)^H\right] \\ &= \mathrm{tr}\left(\mathbf{A}\tilde{\mathbf{U}}\mathbf{V}^H\mathbf{V}\tilde{\mathbf{U}}^H\mathbf{A}^H - \mathbf{R}_d^{\frac{1}{2}}\mathbf{V}\tilde{\mathbf{U}}^H\mathbf{A}^H - \mathbf{A}\tilde{\mathbf{U}}\mathbf{V}^H\mathbf{R}_d^{\frac{1}{2}H} + \mathbf{R}_d\right). \end{aligned}$$

Since

$$\mathbf{A}\tilde{\mathbf{U}}\mathbf{V}^H\mathbf{V}\tilde{\mathbf{U}}^H\mathbf{A}^H = \mathbf{A}\tilde{\mathbf{U}}\mathbf{I}_M\tilde{\mathbf{U}}^H\mathbf{A}^H = \mathbf{V}\tilde{\mathbf{\Sigma}}\tilde{\mathbf{\Sigma}}^H\mathbf{V}^H = \mathbf{V}\tilde{\mathbf{\Sigma}}^2\mathbf{V}^H,$$

then

$$d_{R_2}^2 = \mathrm{tr}\left(\mathbf{V}\tilde{\mathbf{\Sigma}}^2\mathbf{V}^H - \mathbf{R}_d^{\frac{1}{2}}\mathbf{V}\tilde{\mathbf{\Sigma}}^H\mathbf{V}^H - \mathbf{V}\tilde{\mathbf{\Sigma}}\mathbf{V}^H\mathbf{R}_d^{\frac{1}{2}H} + \mathbf{R}_d\right).$$

If $\mathbf{R}_d = \mathbf{I}_M$, then

$$d_{R_2}^2 = \mathrm{tr}\left(\mathbf{V}\tilde{\mathbf{\Sigma}}^2\mathbf{V}^H - 2\mathbf{V}\tilde{\mathbf{\Sigma}}\mathbf{V}^H\right) + M. \tag{3.24}$$

For Euclidean Distance we have

$$\begin{aligned} d_E^2 &= \left\|\mathbf{A}\mathbf{A}^H - \mathbf{R}_d\right\|_2^2 \\ &= \mathrm{tr}\left[\left(\mathbf{A}\mathbf{A}^H - \mathbf{R}_d\right)\left(\mathbf{A}\mathbf{A}^H - \mathbf{R}_d\right)^H\right] \\ &= \mathrm{tr}\left[\mathbf{A}\mathbf{A}^H\mathbf{A}\mathbf{A}^H - \mathbf{R}_d\mathbf{A}\mathbf{A}^H - \mathbf{A}\mathbf{A}^H\mathbf{R}_d^H + \mathbf{R}_d^2\right]. \end{aligned}$$

Since

$$\mathbf{A}\mathbf{A}^H\mathbf{A}\mathbf{A}^H = \mathbf{V}\tilde{\mathbf{\Sigma}}^2\mathbf{V}^H\mathbf{V}\tilde{\mathbf{\Sigma}}^2\mathbf{V}^H = \mathbf{V}\tilde{\mathbf{\Sigma}}^4\mathbf{V}^H,$$

then

$$d_E^2 = \mathrm{tr}\left(\mathbf{V}\tilde{\mathbf{\Sigma}}^4\mathbf{V}^H - \mathbf{R}_d\mathbf{V}\tilde{\mathbf{\Sigma}}^2\mathbf{V}^H - \mathbf{V}\tilde{\mathbf{\Sigma}}^2\mathbf{V}^H\mathbf{R}_d^H + \mathbf{R}_d^2\right).$$

If $\mathbf{R}_d = \mathbf{I}_M$, then

$$d_E^2 = \mathrm{tr}\left(\mathbf{V}\tilde{\mathbf{\Sigma}}^4\mathbf{V}^H - 2\mathbf{V}\tilde{\mathbf{\Sigma}}^2\mathbf{V}^H\right) + M. \tag{3.25}$$

Comparing these two metrics, we have

$$\begin{aligned} d_{R_2}^2 - d_E^2 &= \mathrm{tr}\left(\mathbf{V}\tilde{\mathbf{\Sigma}}^2\mathbf{V}^H - 2\mathbf{V}\tilde{\mathbf{\Sigma}}\mathbf{V}^H\right) - \mathrm{tr}\left(\mathbf{V}\tilde{\mathbf{\Sigma}}^4\mathbf{V}^H - 2\mathbf{V}\tilde{\mathbf{\Sigma}}^2\mathbf{V}^H\right) \\ &= \mathrm{tr}\left(3\mathbf{V}\tilde{\mathbf{\Sigma}}^2\mathbf{V}^H - 2\mathbf{V}\tilde{\mathbf{\Sigma}}\mathbf{V}^H - \mathbf{V}\tilde{\mathbf{\Sigma}}^4\mathbf{V}^H\right) \\ &= \mathrm{tr}\left[\mathbf{V}\left(3\tilde{\mathbf{\Sigma}}^2 - 2\tilde{\mathbf{\Sigma}} - \tilde{\mathbf{\Sigma}}^4\right)\mathbf{V}^H\right] \\ &= \mathrm{tr}\left[\mathbf{V}^H\mathbf{V}\left(3\tilde{\mathbf{\Sigma}}^2 - 2\tilde{\mathbf{\Sigma}} - \tilde{\mathbf{\Sigma}}^4\right)\right] \\ &= \mathrm{tr}\left(3\tilde{\mathbf{\Sigma}}^2 - 2\tilde{\mathbf{\Sigma}} - \tilde{\mathbf{\Sigma}}^4\right). \end{aligned}$$

Suppose $\{a_m\}_{m=1}^M$ are the elements on the diagonal matrix $\tilde{\mathbf{\Sigma}}$, then

$$\mathrm{tr}\left(3\tilde{\mathbf{\Sigma}}^2 - 2\tilde{\mathbf{\Sigma}} - \tilde{\mathbf{\Sigma}}^4\right) = \sum_{m=1}^{M}\left(3a_m^2 - 2a_m - a_m^4\right) = \sum_{m=1}^{M}\left[-(a_m-1)^2(a_m+2)a_m\right].$$

For $a_m > 0$, $3a_m^2 - 2a_m - a_m^4 < 0$. Then, $d_{R_2}^2 - d_E^2 < 0$. In the case when $\mathbf{R}_d = \mathbf{I}_M$, we will have $d_{R_2}^2 < d_E^2$.

Now, we will show how $d_{R_2}^2$ and d_E^2 can be quadratic in $\mathbf{A}$.

$$\begin{aligned} d_{R_2}^2 &= \left\|\mathbf{A}\tilde{\mathbf{U}}_{n-1}\mathbf{V}_{n-1}^H - \mathbf{R}_d^{\frac{1}{2}}\right\|_2^2 \\ &= \mathrm{tr}\left[\left(\mathbf{A}\tilde{\mathbf{U}}_{n-1}\mathbf{V}_{n-1}^H - \mathbf{R}_d^{\frac{1}{2}}\right)\left(\mathbf{A}\tilde{\mathbf{U}}_{n-1}\mathbf{V}_{n-1}^H - \mathbf{R}_d^{\frac{1}{2}}\right)^H\right] \\ &= \mathrm{tr}\left(\mathbf{A}\tilde{\mathbf{U}}_{n-1}\mathbf{V}_{n-1}^H\mathbf{V}_{n-1}\tilde{\mathbf{U}}_{n-1}^H\mathbf{A}^H - \mathbf{R}_d^{\frac{1}{2}}\mathbf{V}_{n-1}\tilde{\mathbf{U}}_{n-1}^H\mathbf{A}^H - \mathbf{A}\tilde{\mathbf{U}}_{n-1}\mathbf{V}_{n-1}^H\mathbf{R}_d^{\frac{1}{2}H} + \mathbf{R}_d\right) \\ &= \mathrm{vec}^H(\mathbf{A})\left[\left(\tilde{\mathbf{U}}_{n-1}\mathbf{V}_{n-1}^H\mathbf{V}_{n-1}\tilde{\mathbf{U}}_{n-1}^H\right)^T \otimes \mathbf{I}_M\right]\mathrm{vec}(\mathbf{A}) \\ &\quad - \mathrm{vec}^H(\mathbf{A})\mathrm{vec}\left(\mathbf{R}_d^{\frac{1}{2}}\mathbf{V}_{n-1}\tilde{\mathbf{U}}_{n-1}^H\right) - \mathrm{vec}^H\left(\mathbf{R}_d^{\frac{1}{2}}\mathbf{V}_{n-1}\tilde{\mathbf{U}}_{n-1}^H\right)\mathrm{vec}(\mathbf{A}) + \mathrm{tr}(\mathbf{R}_d), \end{aligned}$$

and

$$\begin{aligned} d_E^2 &= \left\| \mathbf{A}\mathbf{A}_{n-1}^H - \mathbf{R}_d \right\|_2^2 \\ &= \mathrm{tr}\left[\left(\mathbf{A}\mathbf{A}_{n-1}^H - \mathbf{R}_d \right) \left(\mathbf{A}\mathbf{A}_{n-1}^H - \mathbf{R}_d \right)^H \right] \\ &= \mathrm{vec}^H(\mathbf{A}) \left[\left(\mathbf{A}_{n-1}^H \mathbf{A}_{n-1} \right)^T \otimes \mathbf{I}_M \right] \mathrm{vec}(\mathbf{A}) \\ &- \mathrm{vec}^H(\mathbf{A}) \mathrm{vec}\left(\mathbf{R}_d \mathbf{A}_{n-1} \right) - \mathrm{vec}^H\left(\mathbf{R}_d \mathbf{A}_{n-1} \right) \mathrm{vec}(\mathbf{A}) + \mathrm{tr}(\mathbf{R}_d \mathbf{R}_d^H). \end{aligned}$$

Similarly, the constraint is quadratic in $\mathbf{A}$, such that

$$\begin{aligned} \left\| \mathbf{A}\mathbf{\Phi}^T(\tau)\mathbf{A}_{n-1}^H \right\|^2 &= \mathrm{tr}\left[\mathbf{A}\mathbf{\Phi}^T(\tau)\mathbf{A}_{n-1}^H \mathbf{A}_{n-1}\mathbf{\Phi}^*(\tau)\mathbf{A}^H \right] \\ &= \mathrm{vec}^H(\mathbf{A}) \left[\left(\mathbf{\Phi}^T(\tau)\mathbf{A}_{n-1}^H \mathbf{A}_{n-1}\mathbf{\Phi}^*(\tau) \right)^T \otimes \mathbf{I}_M \right] \mathrm{vec}(\mathbf{A}). \end{aligned}$$

Therefore, the problem could be solved by the standard optimization tools (such as CVX [26]).

Chapter 4

Numerical Experiments

In this chapter, we show examples for illustrating the performance of our proposed method described in Chapter 3. In this minimization problem, suppose that the length of the waveform is $64ms$. Walsh function is used as the orthonormal basis in this minimization problem, and the number of orthonormal basis vectors is $K = 32$. The desired covariance matrix $\mathbf{R}_d$ is an $M \times M$ identity matrix. In the first part, we synthesize the signal sequences with different numbers of antennas. In the second part, we use one of the synthesized signal sequences in an application to detect targets.

4.1 Optimization Results of Waveform Synthesis with Riemannian Distance

We can offer some flexibility on the constraints in the minimization problem (3.21). For instance, choose $\varepsilon_1 = \alpha B$ when $\tau = 1$, and $\varepsilon_\tau = \delta B$ when $\tau > 1$, that is

$$\begin{aligned} \left\| \mathbf{A}\mathbf{\Phi}^T(\tau)\mathbf{A}_{n-1}^H \right\|^2 &\leq \alpha B, \ \tau = 1, \\ \left\| \mathbf{A}\mathbf{\Phi}^T(\tau)\mathbf{A}_{n-1}^H \right\|^2 &\leq \delta B, \ \tau > 1, \end{aligned} \tag{4.1}$$

in which αB is larger than δB, but smaller than the trace of $\mathbf{R}_d$. αB defines the slope of the sequence pattern and δB defines the sidelobe levels. In our problem, B is set to be the trace of $\mathbf{R}_d$. Figure 4.1 is a diagram of the specifications against τ.

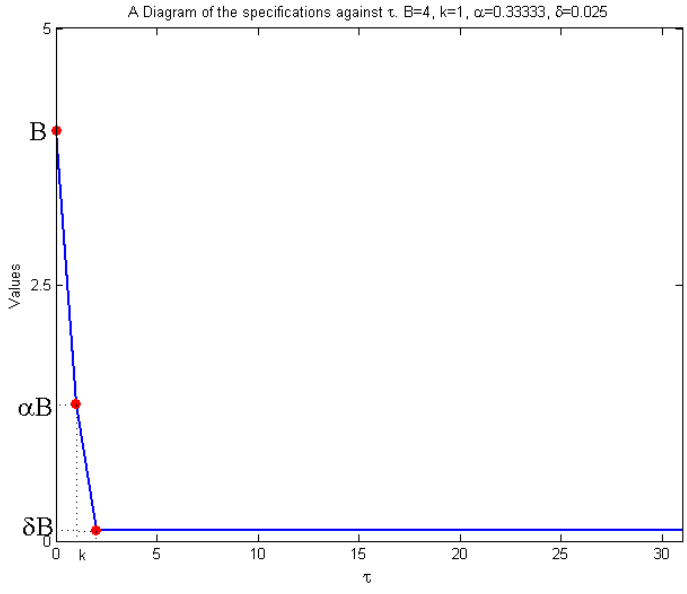

Figure 4.1: A Diagram of the Specifications

Walsh functions are used to synthesize the orthonormal basis matrix $\mathbf{S}$. The Walsh function [27, 28] of order N consists an ordered set of N rectangular waveforms taking only two amplitude values $+1$ and -1 over a limited time interval T. These waveforms are denoted as $\{W_j(t),\ t \in (0, T),\ j = 0,\ 1,\ \ldots,\ N-1\}$. [29] It has several properties, such that

- $W_j(t)$ takes on the values $\{1,\ -1\}$;
- $W_0(t) = 1$ for all t in the interval $(0,\ T)$;
- $W_j(t)$ has precisely j sign changes (zero crossings) in the interval $(0,\ T)$;
- $\{W_j(t)\}$ are orthonormal, which means $\frac{1}{T}\int_0^T W_j(t)W_k(t)dt = \delta_{jk}$.

Figure 4.2 shows the first four of the Walsh functions.

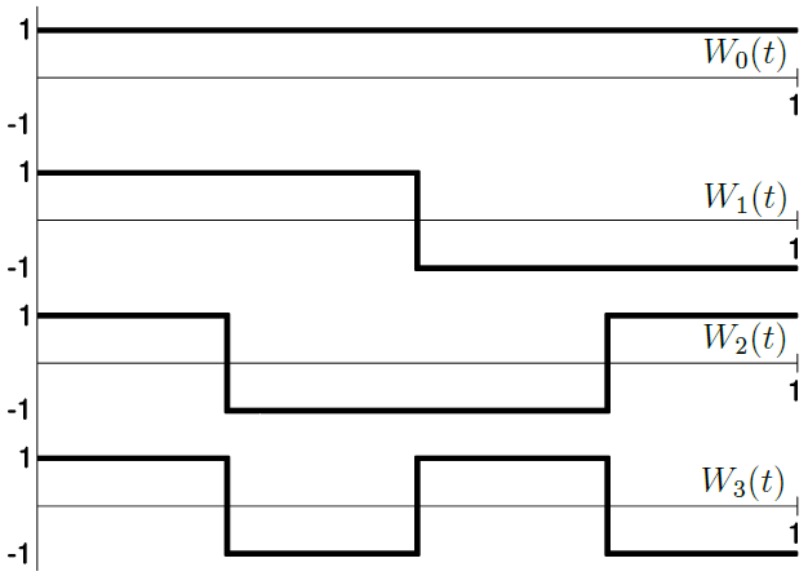

Figure 4.2: The First Four Walsh Functions

Figure 4.3 shows the 32 sequences of the orthonormal bases from the Walsh functions used in the signal synthesis.

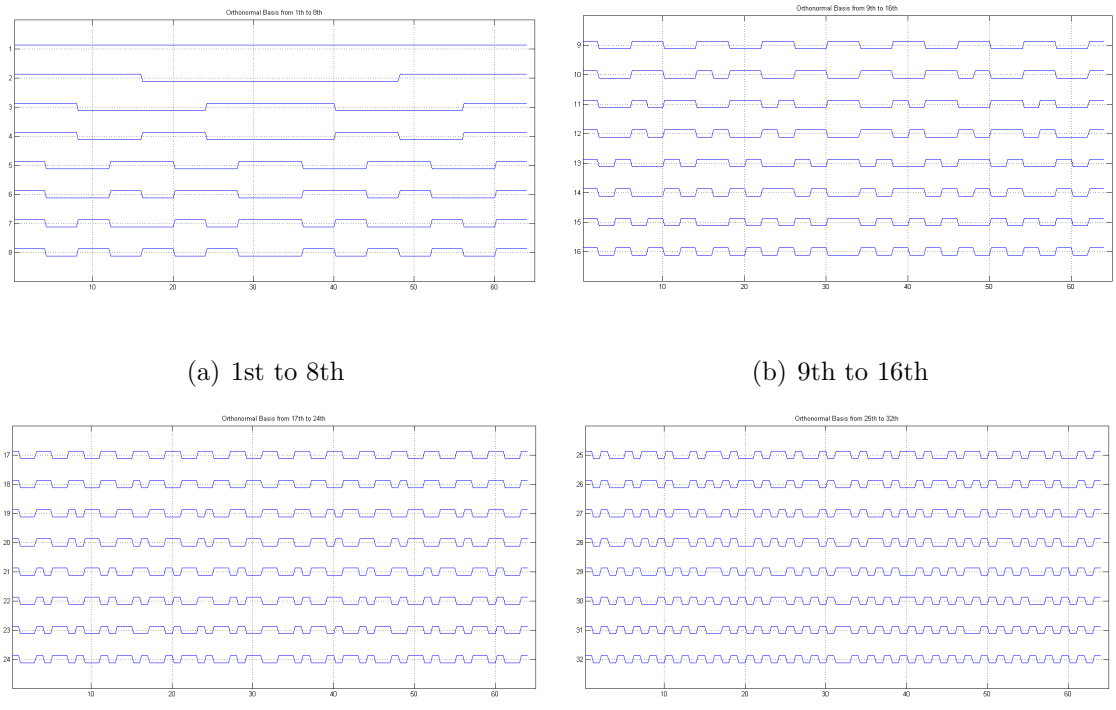

(a) 1st to 8th

(b) 9th to 16th

(c) 17th to 24th

(d) 25th to 32nd

Figure 4.3: Orthonormal Basis

Because of the different Riemannian metrics used in measuring matrix differences, we can formulate this minimization problem with two different objective functions by using the first RD and the second RD. Since $\mathbf{R}_d$ is chosen as an M-by-M identity matrix in our problem, the first RD d_{R_1} equals to the second RD d_{R_2}.

In our problem, we define a merit factor D_i to compare the results by using RD with those using ED. Given the correlation matrix of the transmitted signals in (3.10),

D_i is given by

$$D_i = \frac{|r_{ii}(0)|}{\max_{i \neq j, \tau \neq 0} |r_{ij}(\tau)|}, \tag{4.2}$$

in which i is the ith antenna, and $i \neq j$ when $\tau = 0$. $r_{ii}(0)$ is the autocorrelation coeffcient on the main-diagonal of the covariance matrix $\mathbf{R}_0$, and $r_{ij}(\tau)$ is the correlation coeffcient of the correlation matrix $\mathbf{R}_\tau$ excluding $r_{ii}(0)$. If the transmitted signals have good auto-correlation properties, we can expect the values of $r_{ii}(0)$ to be 1 (as the desired covariance matrix $\mathbf{R}_d$ in our case) and the values of $r_{ij}(0)$ to be as small as possible. Then this merit factor D_i will be large.

Now, referring to the minimization problem formulated in (3.21), we specify our problem by several groups of parameters, which is represented as (M, α, δ), in which M is the antenna number, α and δ are the scalars in the constraints. The parameter groups used are listed as $(3, 0.1216, 0.0167)$, $(4, 0.1727, 0.0232)$, $(5, 0.2657, 0.0293)$, and $(6, 0.3170, 0.0364)$. First of all, using the standard optimization tools (CVX [26]) for solving the problem, we show the values of the difference between the covariance matrix of the synthesized signals and the desired covariance matrix by using the metric of RD and the metric of ED separately in Table 4.1. We also compare them by setting the numbers of orthonormal basis K as 32 and 48 separately. Within the same iteration period, by using RD, the synthesized signals can satisfy the defined requirements more precisely.

- *cvx_optval* contains the value of the objective function;
- The *cvx_status* is "solved" in each condition;
- d_E^2 is defined in Eq.(3.22), and d_{R2}^2 is defined in Eq.(3.20).

Table 4.1: The Last Values of Difference in Each Condition

Orthonormal Basis K	(M, α, δ)	Iteration Period	**A** synthesized by using RD		**A** synthesized by using ED	
			$d_{R_2} = \left\|\mathbf{A}\tilde{\mathbf{U}}\mathbf{V}^H - \mathbf{R}_d^{1/2}\right\|_2$	$d_E = \left\|\mathbf{A}\mathbf{A}^H - \mathbf{R}_d\right\|_2$	$d_{R_2} = \left\|\mathbf{A}\tilde{\mathbf{U}}\mathbf{V}^H - \mathbf{R}_d^{1/2}\right\|_2$	$d_E = \left\|\mathbf{A}\mathbf{A}^H - \mathbf{R}_d\right\|_2$
32	(3, 0.1216, 0.0167)	100	1.5529E-09	3.1058E-09	2.9200E-02	5.8500E-02
	(4, 0.1727, 0.0232)	100	5.3257E-10	1.0651E-09	4.2700E-02	8.5500E-02
	(5, 0.2657, 0.0293)	200	2.1425E-09	4.2851E-09	5.6600E-02	1.1310E-01
	(6, 0.3170, 0.0364)	280	7.2138E-10	1.4428E-09	4.8900E-02	9.7600E-02
48	(3, 0.1770, 0.0207)	100	1.7466E-09	3.4933E-09	2.6800E-02	5.3700E-02
	(4, 0.2589, 0.0347)	100	1.8127E-09	3.6254E-09	3.5400E-02	7.0800E-02
	(5, 0.3977, 0.0439)	200	1.0252E-10	2.0503E-10	5.4300E-02	1.0700E-01
	(6, 0.4754, 0.0545)	280	6.4561E-11	1.2912E-10	5.9900E-02	1.2040E-01

Secondly, Figure 4.4 displays the designed signal sequences with different antenna number. Table 4.2 contains the values of coefficient matrix **A** (3.6) when $M = 3$.

Table 4.2: The Coefficient Matrix when $M = 3$

	RD			ED		
M=3	1st	2nd	3rd	1st	2nd	3rd
K=32 Orthonormal Basis	0.1237	-0.0629	0.1916	0.0377	-0.0973	0.2012
	-0.2766	0.0914	0.1217	-0.3136	0.2277	0.0919
	-0.3374	0.0795	0.0891	-0.3588	0.0895	0.1384
	-0.1769	-0.0592	0.2259	-0.1457	-0.0241	0.1742
	-0.2376	-0.1010	-0.2163	-0.2379	-0.0601	-0.2484
	-0.1118	-0.1032	-0.0296	-0.1387	-0.0986	-0.0716
	0.0218	-0.2038	-0.1167	0.0271	-0.2104	-0.2087
	-0.0697	0.0715	0.0118	-0.0189	-0.0541	0.0948
	-0.2543	-0.1202	0.0514	-0.2844	-0.1045	0.0279
	0.2164	0.2458	-0.1443	0.2493	0.2174	-0.1151
	0.1117	-0.2221	0.2904	0.1851	-0.2102	0.2469
	0.3783	-0.2087	-0.2362	0.4257	-0.1618	-0.2518
	0.0818	-0.2053	0.0921	0.1506	-0.1892	0.1490
	-0.2407	0.0132	0.2562	-0.1504	-0.0034	0.2410
	-0.0867	-0.0814	0.0756	0.0442	-0.0838	0.0540
	0.0627	-0.2895	0.1119	0.1350	-0.3184	0.1376
	0.2844	0.0541	0.1585	0.2453	0.1328	0.1431
	0.2073	0.1084	0.1785	0.1624	0.0863	0.1612
	0.1052	0.3464	-0.0105	0.1251	0.3622	-0.0616
	0.0741	-0.0983	0.3055	0.0698	-0.0578	0.2199
	0.1497	0.1863	-0.0957	0.1536	0.1810	-0.1823
	0.2490	0.0759	0.0191	0.0829	0.1292	-0.0675
	-0.1536	0.2356	0.0218	-0.1099	0.1551	0.0850
	-0.0633	0.1319	-0.2136	-0.0174	0.0656	-0.1673
	-0.0787	0.1209	0.2551	0.0278	0.2111	0.1529
	-0.0029	-0.1117	0.0270	-0.0399	-0.1964	0.1711
	-0.0440	0.2141	-0.0127	-0.1564	0.1293	-0.0078
	-0.0286	-0.4008	-0.2302	-0.1086	-0.4421	-0.2163
	0.0620	0.2237	0.2426	0.0855	0.0526	0.2427
	-0.0047	0.0297	-0.2874	0.0557	-0.0353	-0.1957
	-0.1885	0.1977	-0.3157	-0.1504	0.2025	-0.3567
	0.2116	0.1691	0.0777	0.2004	0.1729	0.1515

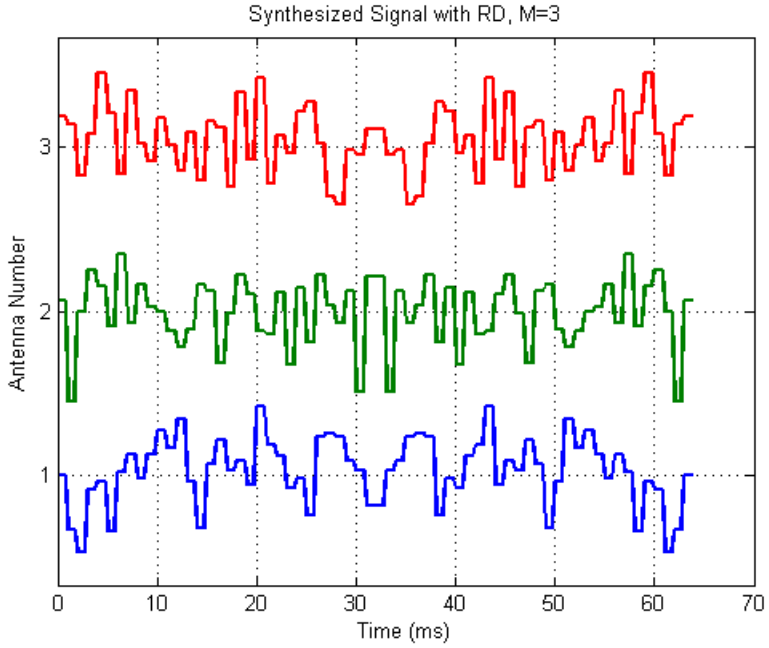
Synthesized Signal with RD, M=3
Antenna Number
Time (ms)
1
2
3
0
10
20
30
40
50
60
70

(a) RD, $M = 3$

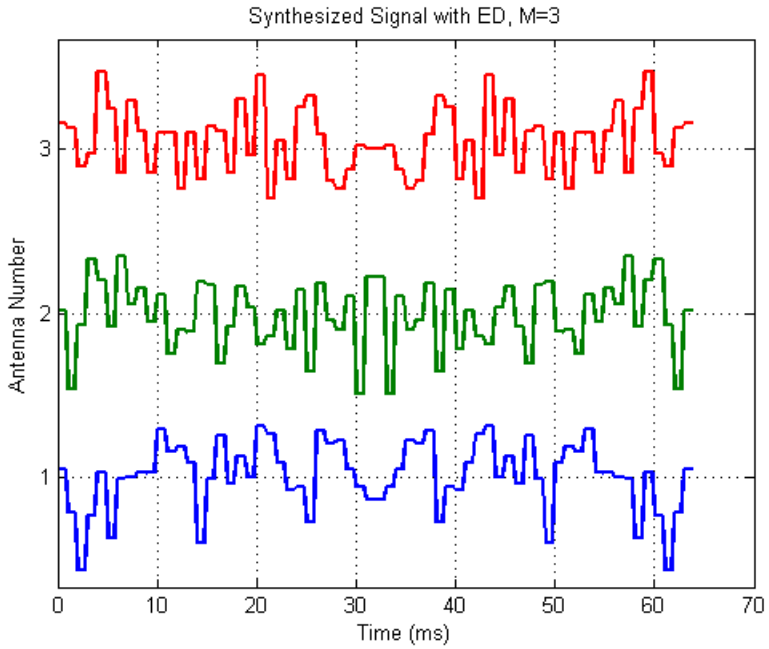
Synthesized Signal with ED, M=3
Antenna Number
Time (ms)
1
2
3
0
10
20
30
40
50
60
70

(b) ED, $M = 3$

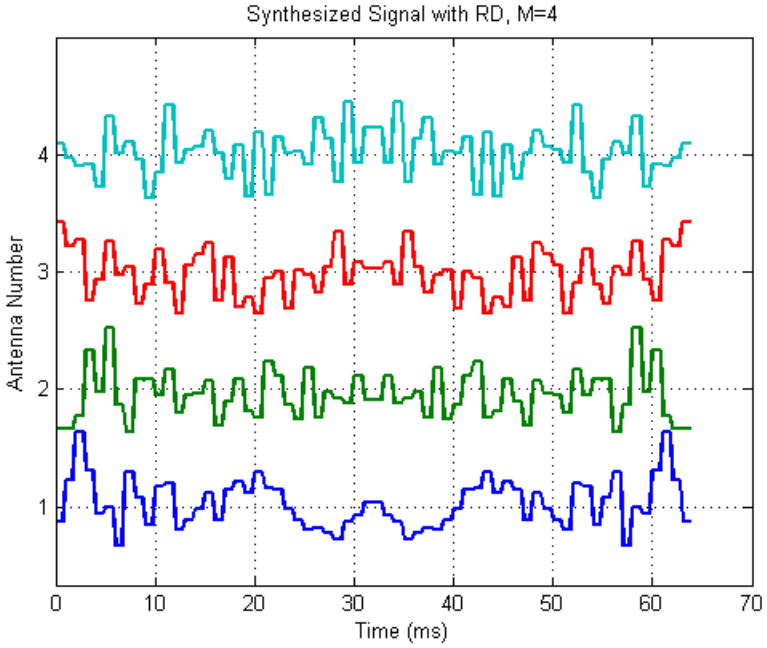
Synthesized Signal with RD, M=4
Antenna Number
Time (ms)
1
2
3
4
0
10
20
30
40
50
60
70

(c) RD, $M = 4$

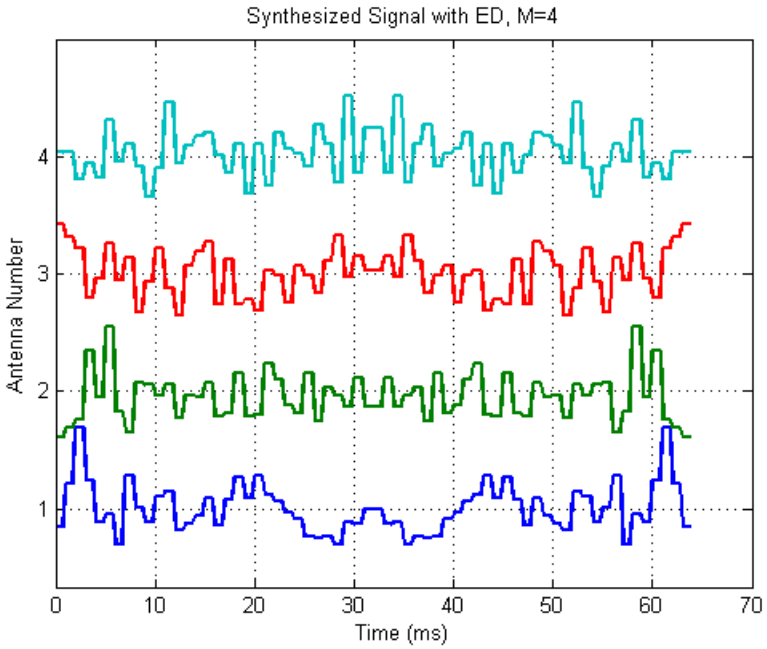
Synthesized Signal with ED, M=4
Antenna Number
Time (ms)
1
2
3
4
0
10
20
30
40
50
60
70

(d) ED, $M = 4$

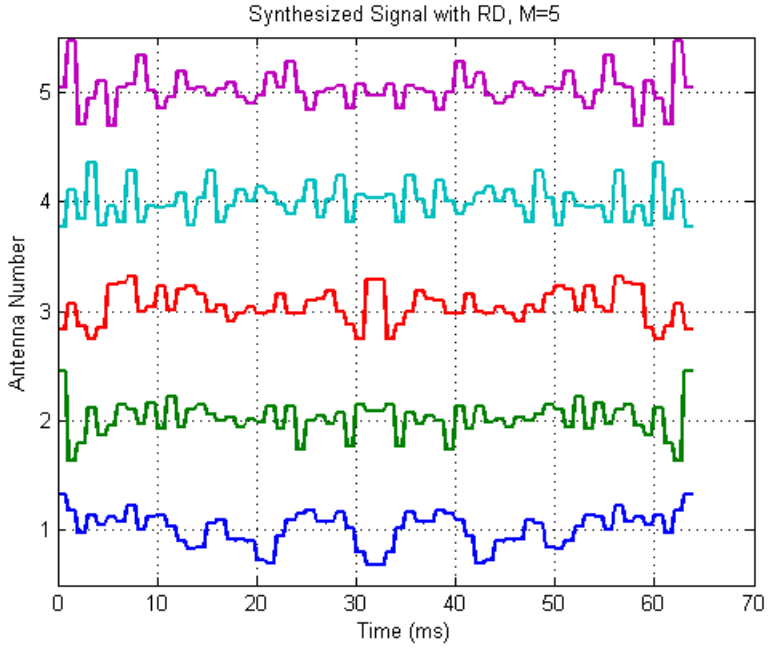
Synthesized Signal with RD, M=5
Antenna Number
Time (ms)
1
2
3
4
5
0
10
20
30
40
50
60
70

(e) RD, $M = 5$

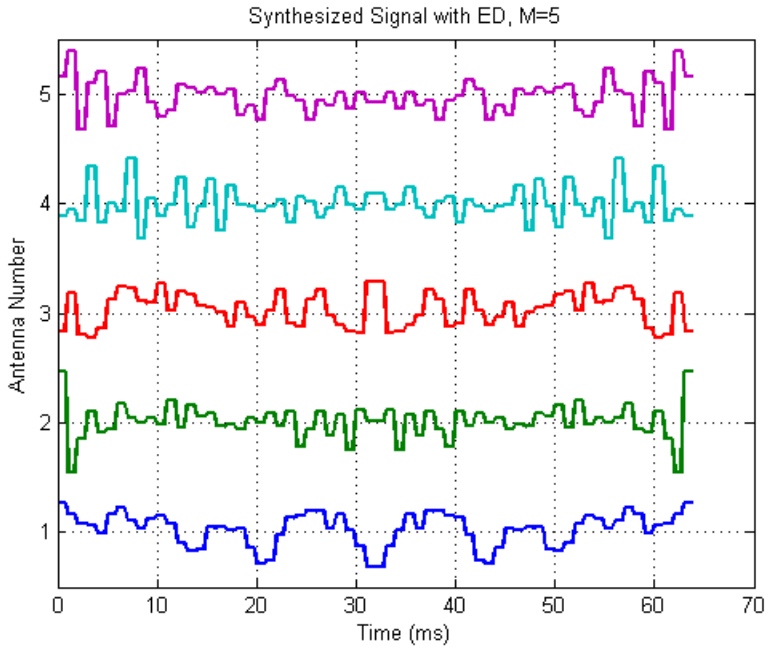
Synthesized Signal with ED, M=5
Antenna Number
Time (ms)
1
2
3
4
5
0
10
20
30
40
50
60
70

(f) ED, $M = 5$

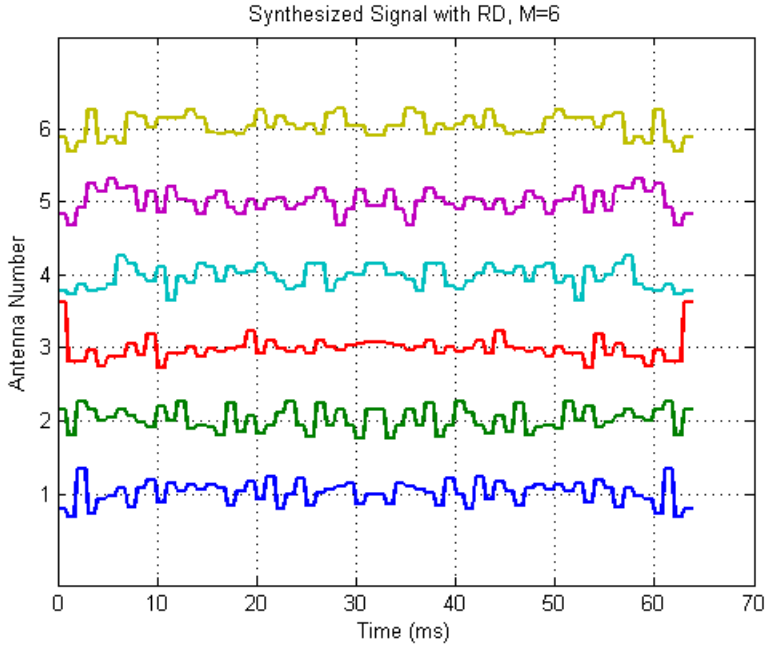

(g) RD, $M = 6$

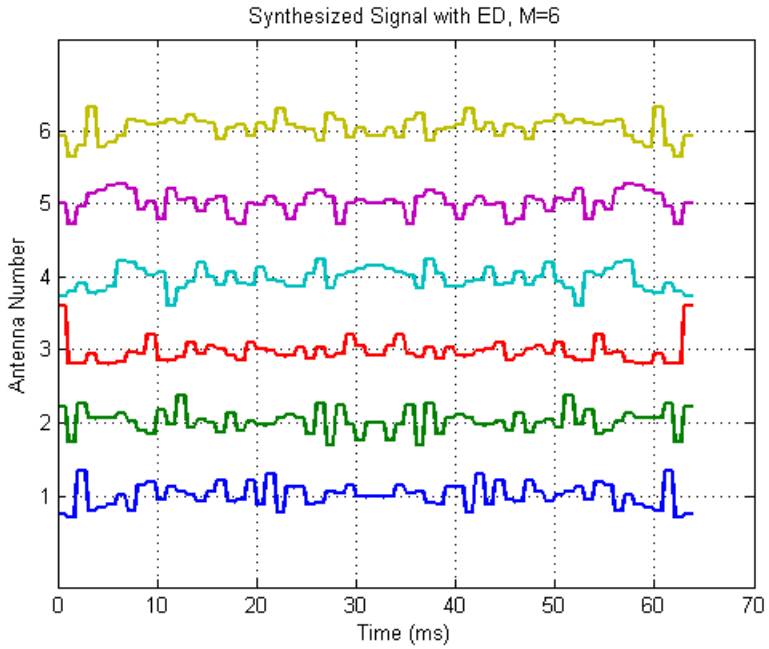

(h) ED, $M = 6$

Figure 4.4: Synthesized Signals

The results for the merit factor D_i (4.2) are shown in Figure 4.5, which compares the correlation properties of every sensor measured by RD and ED. The corresponding numerical values are listed in Table 4.3. We can observe that most of the values of D_i with RD are higher than those with ED after the same iteration period. The reason why the D_i values of ED fluctuate might be that ED has not converged while RD has reached an optimum value.

Table 4.3: The Values of D_i

(M, α, δ)	D_i	1	2	3	4	5	6
(3, 0.1216, 0.0167)	RD	2.7581	2.7581	2.7581	—	—	—
	ED	3.0902	3.0849	2.9815	—	—	—
(4, 0.1727, 0.0232)	RD	2.6540	2.6540	2.6540	2.6540	—	—
	ED	2.6049	2.5868	2.5708	2.5189	—	—
(5, 0.2657, 0.0293)	RD	1.6570	1.6570	1.6570	1.6570	1.6570	—
	ED	1.5051	1.5400	1.5685	1.6526	1.6016	—
(6, 0.3170, 0.0364)	RD	2.2893	2.2893	2.2893	2.2893	2.2893	2.2893
	ED	2.7611	2.1437	2.1696	2.1080	2.1004	2.1418

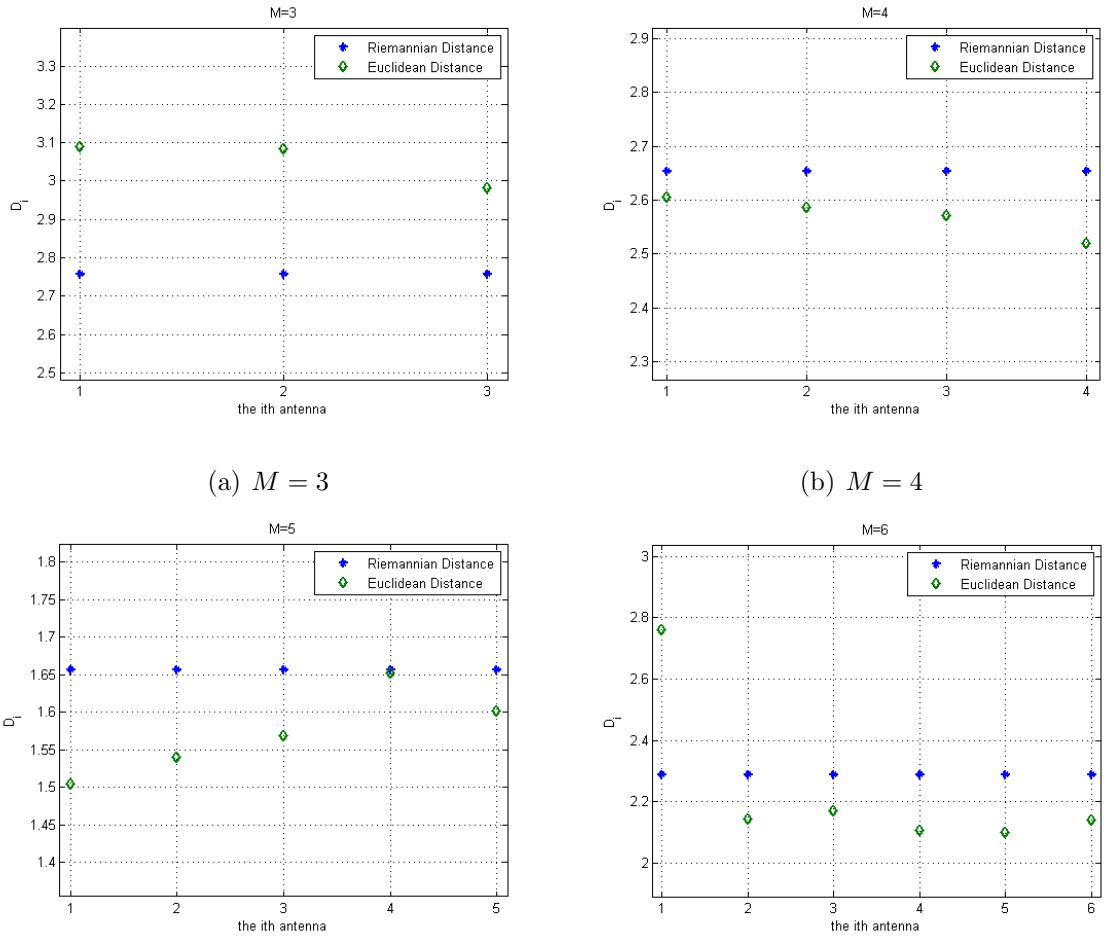

(a) $M = 3$ (b) $M = 4$

(c) $M = 5$ (d) $M = 6$

Figure 4.5: the Values of Each D_i

Figures 4.6, 4.7 and 4.8 show the values of $\mathbf{R}_0$, $\mathbf{R}_1$, and the average values of $\mathbf{R}_\tau$ with $\tau > 1$, which illustrate the synthesized-signals' ability of satisfying the defined correlation requirements. All the corresponding values are listed in Table 4.4.

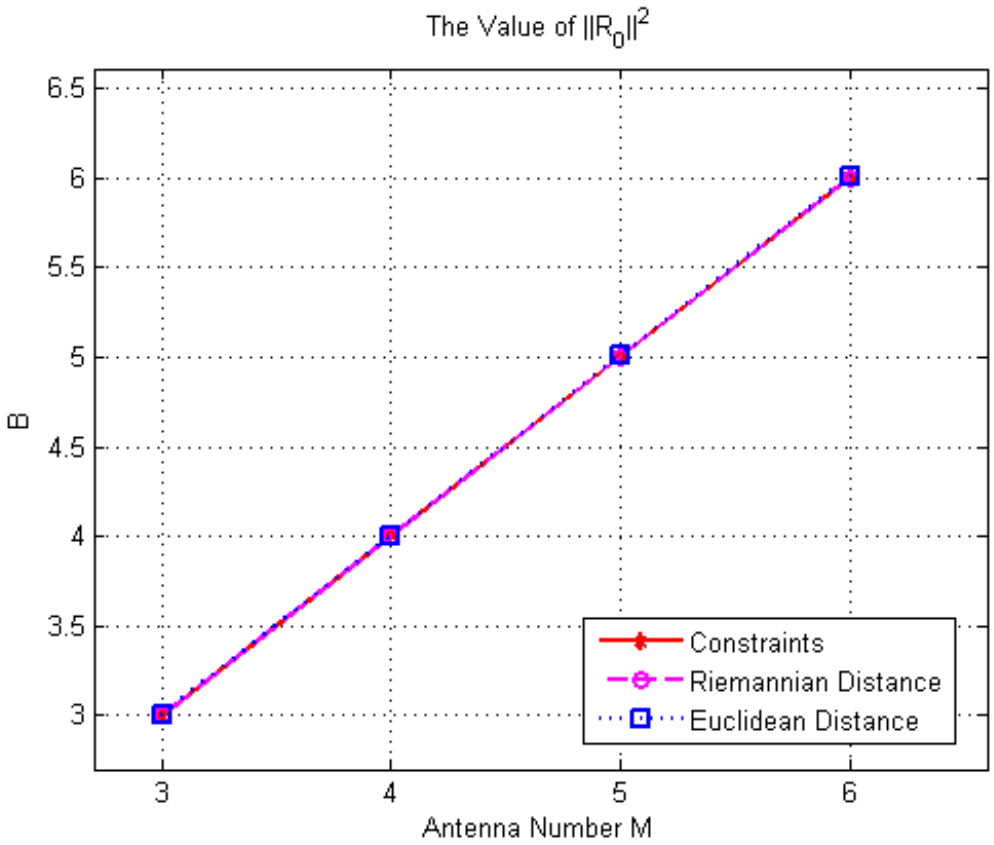

Figure 4.6: The Value of $\mathbf{R}_0$

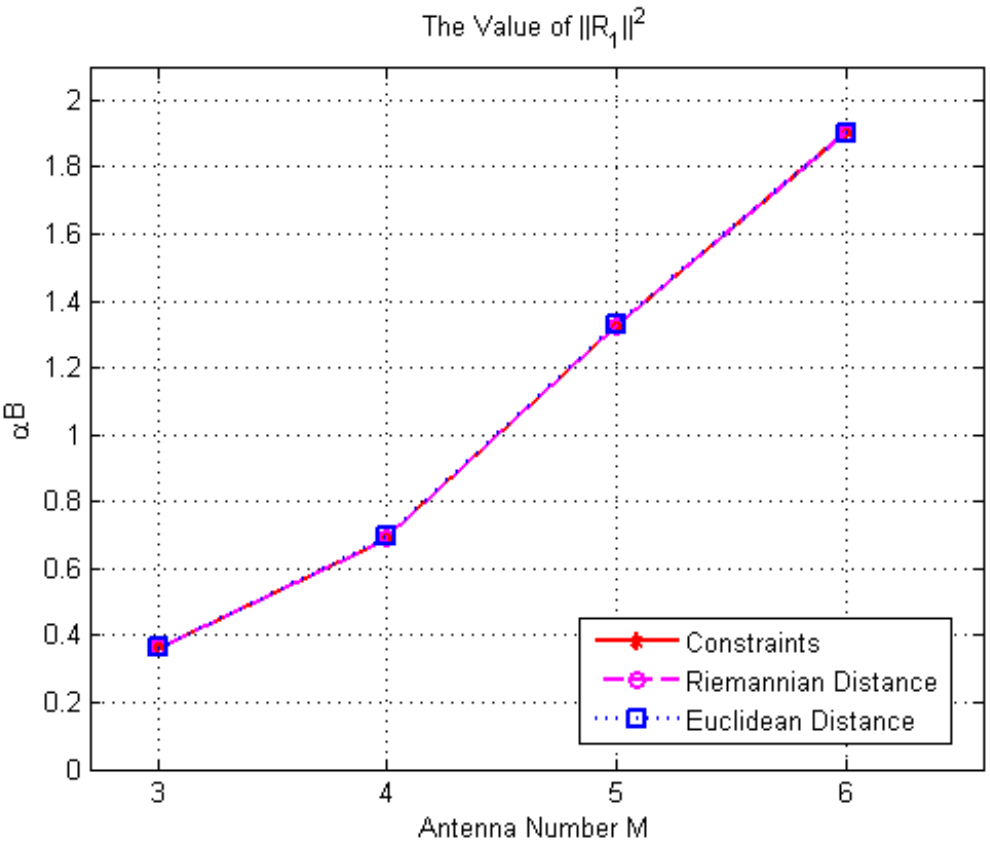

Figure 4.7: The Value of $\mathbf{R}_1$

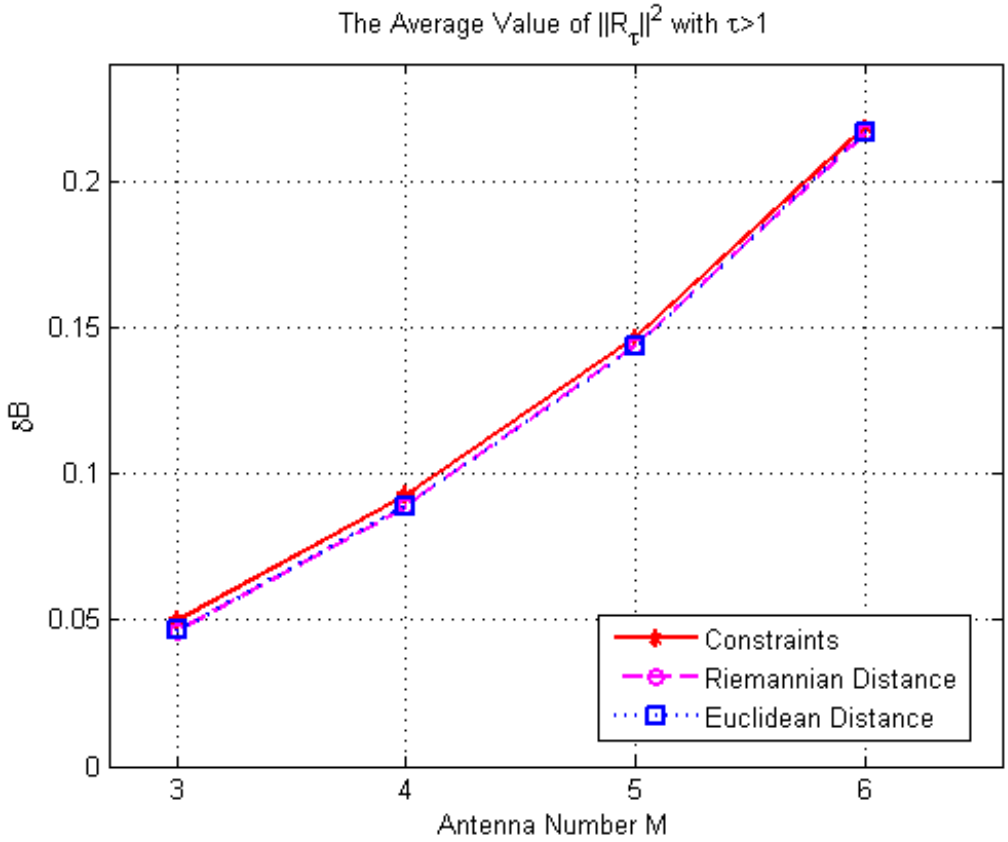

Figure 4.8: The Value of $\mathbf{R}_\tau$ with $\tau > 1$.

Table 4.4: The Values of $\mathbf{R}_\tau$

(M, α, δ)		$\|\|R(0)\|\|^2$	$\|\|R(1)\|\|^2$	avg ($\|\|R(\tau)\|\|^2$), $\tau > 1$
(3, 0.1216, 0.0167)	Constraints	3.0000	0.3647	0.0500
	RD	3.0000	0.3646	0.0460
	ED	3.0034	0.3642	0.0464
(4, 0.1727, 0.0232)	Constraints	4.0000	0.6906	0.0927
	RD	4.0000	0.6904	0.0887
	ED	4.0073	0.6966	0.0890
(5, 0.2657, 0.0293)	Constraints	5.0000	1.3255	0.1463
	RD	5.0000	1.3241	0.1437
	ED	5.0128	1.3293	0.1433
(6, 0.3170, 0.0364)	Constraints	6.0000	1.9017	0.2182
	RD	6.0000	1.9014	0.2162
	ED	6.0095	1.9040	0.2167

Furthermore, we can compare the autocorrelation of each antenna without time shift, that is, $r_{ii}(0)$, as shown in Figure 4.9. The corresponding values are listed in Table 4.5.

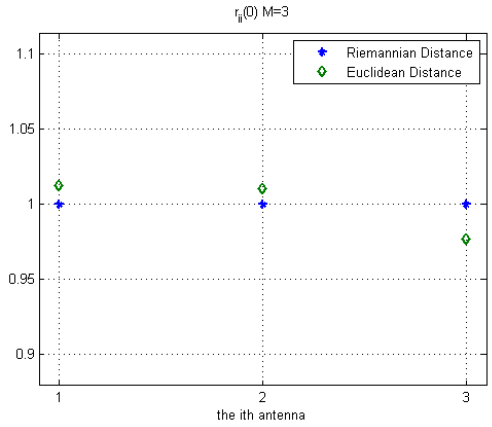

(a) $M = 3$

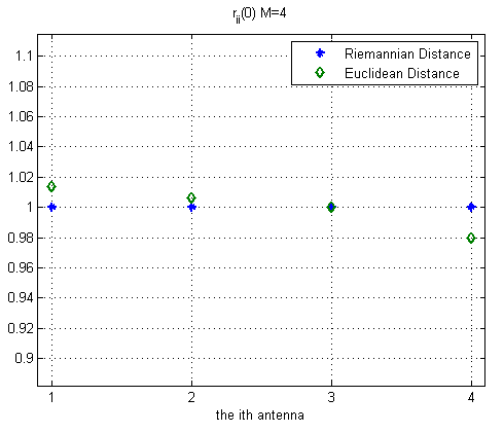

(b) $M = 4$

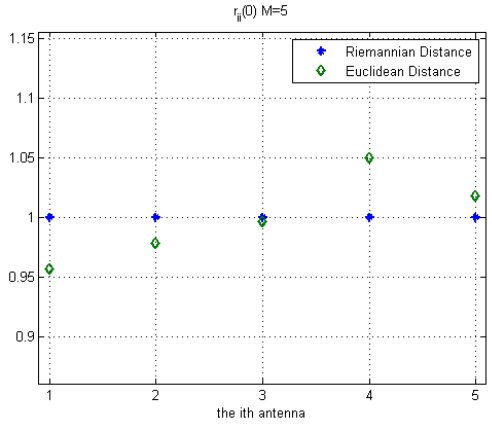

(c) $M = 5$

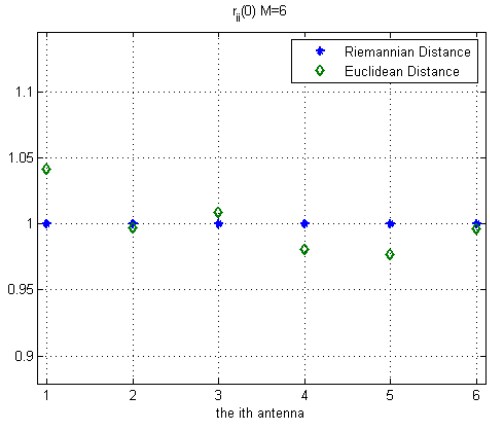

(d) $M = 6$

Figure 4.9: the Values of Each $r_{ii}(0)$

Table 4.5: The Values of $r_{ii}(0)$

(M, α, δ)	$r_{ii}(0)$	1	2	3	4	5	6
(3, 0.1216, 0.0167)	RD	1.0000	1.0000	1.0000	—	—	—
	ED	1.0125	1.0107	0.9768	—	—	—
(4, 0.1727, 0.0232)	RD	1.0000	1.0000	1.0000	1.0000	—	—
	ED	1.0135	1.0064	1.0002	0.9800	—	—
(5, 0.2657, 0.0293)	RD	1.0000	1.0000	1.0000	1.0000	1.0000	—
	ED	0.9565	0.9786	0.9968	1.0502	1.0178	—
(6, 0.3170, 0.0364)	RD	1.0000	1.0000	1.0000	1.0000	1.0000	1.0000
	ED	1.0412	0.9969	1.0089	0.9803	0.9767	0.9960

From the above figures and tables, we can see that the synthesized signals from the two methods possess good auto-correlation properties and cross-correlation properties.

4.2 Detection by Using the Synthesized Waveforms

With the synthesized transmitted signals, we can further our problem to the detection of targets. In this part, we simulate the environment where there exists an additive white Gaussian noise. Suppose that the transmitted signals last for $64ms$, which are transmitted at the speed of $c = 3 \times 10^8 m/s$ in the space. The transmitter and the receiver in the MIMO radar are equipped with $M = 6$ antennas (uniform linear array and half wavelength inter-element spacing), and the sampling rate is 64 $samples/ms$.

- Example 1.1: 3 targets at $(17ms, 15^o)$, $(18.5ms, 15^o)$, $(20ms, 15^o)$, $SNR = -10dB$ in Figure 4.10;
- Example 1.2: 3 targets at $(17ms, 15^o)$, $(18.5ms, 15^o)$, $(20ms, 15^o)$, $SNR = 0dB$ in Figure 4.11;
- Example 1.3: 3 targets at $(17ms, 15^o)$, $(18.25ms, 15^o)$, $(19.5ms, 15^o)$, $SNR = 0dB$ in Figure 4.12.

The numbers on the horizontal line of the following 4 figures denote the angles in degree.

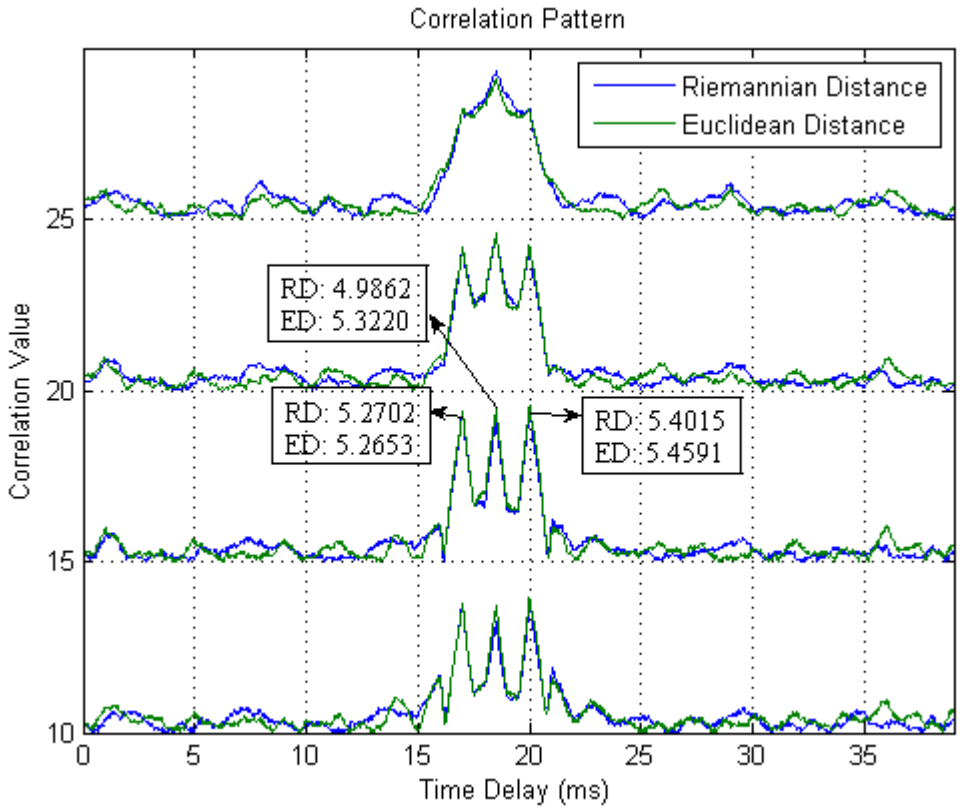

Figure 4.10: Correlation Pattern of Example 1.1, $SNR = -10dB$, 10^o to 25^o, with the Locations $(17ms, 15^o)$, $(18.5ms, 15^o)$, $(20ms, 15^o)$.

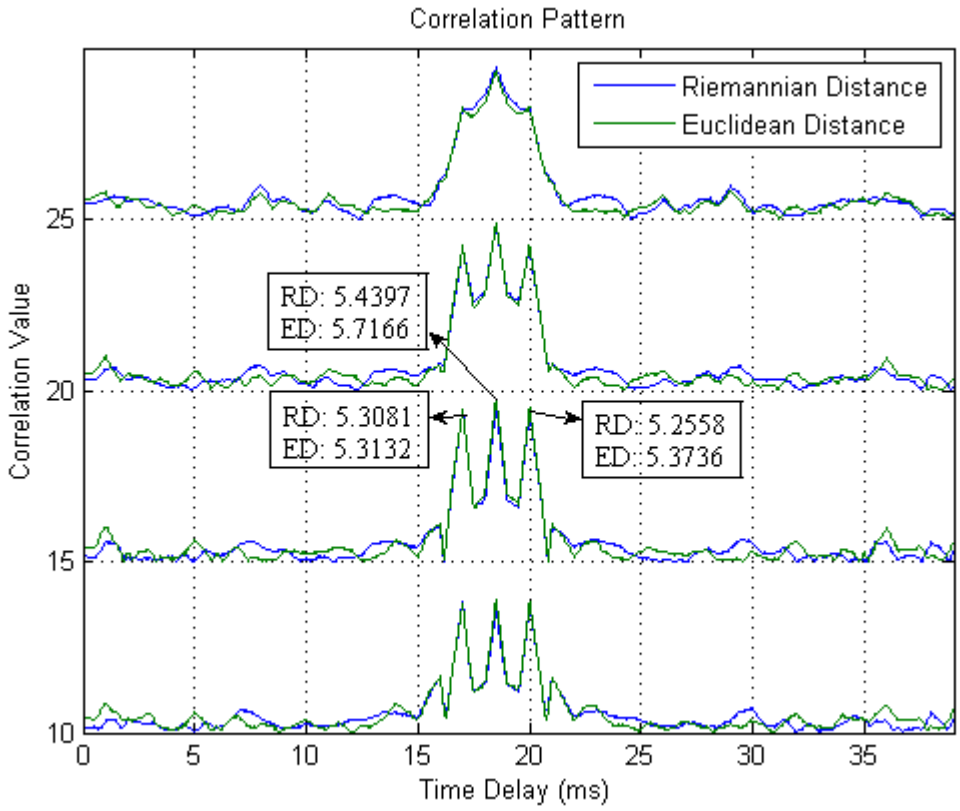

Figure 4.11: Correlation Pattern of Example 1.2, $SNR = 0dB$, 10^o to 25^o, with the Locations $(17ms, 15^o)$, $(18.5ms, 15^o)$, $(20ms, 15^o)$.

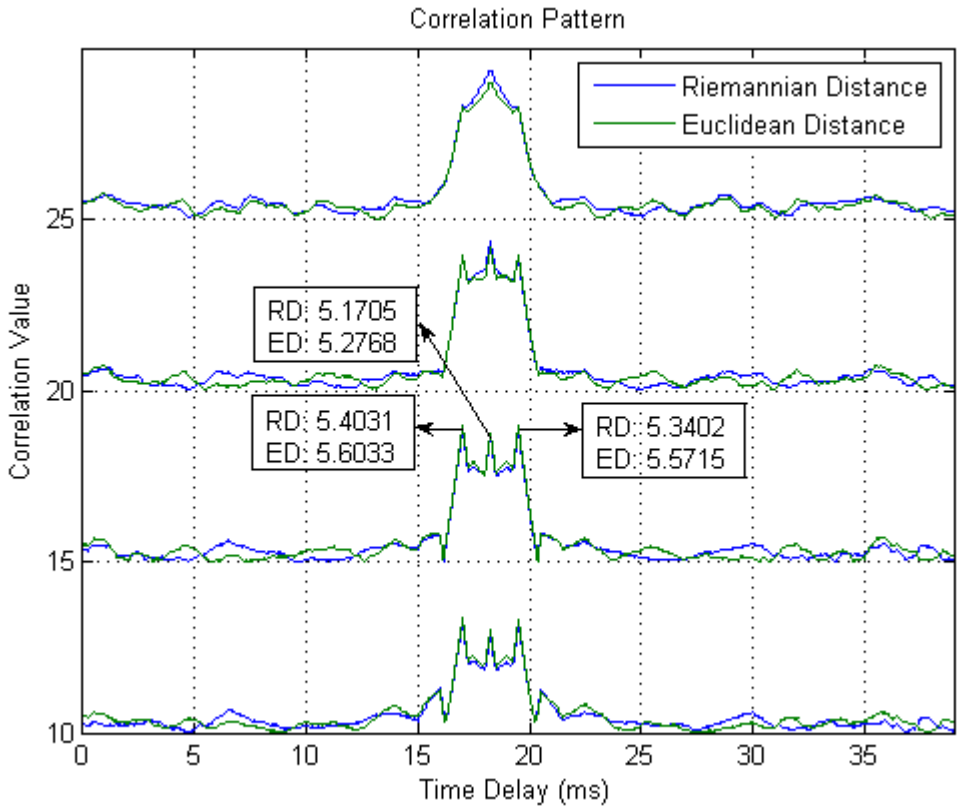

Figure 4.12: Correlation Pattern of Example 1.3, $SNR = 0dB$, 10^o to 25^o, with the Locations $(17ms, 15^o)$, $(18.25ms, 15^o)$, $(19.5ms, 15^o)$.

From the above figures, the trough between the two peak values in RD is slightly wider and deeper than that in ED, which poses a potential advantage in target detection.

Chapter 5

Conclusion and Future Work

In this thesis we examine the signal design problem for Multiple Input Multiple Output (MIMO) radar focusing on matching a desired covariance matrix and on the suppression of the auto-correlation and cross-correlation sidelobes. Furthermore, by reasoning that the estimated covariance matrix of the transmitted signals is Hermitian and positive definite, thereby forming a manifold in the signal space, we use the measure of RD for this estimation error instead of the commonly used ED in the formulation of our problem. Applying this measure to our design objective function, we transform the design into a convex optimization problem, the solution of which can be obtained efficiently by using the standard optimization methods. Although the results don't show that the performance of our design is significantly better than that of using ED in detection in the real application, but with RD, the synthesized signals can satisfy the defined requirements more precisely.

In this thesis, we propose to apply the Walsh functions to the orthonormal bases in our problem. However, there are some other kinds of orthonormal functions with their own advantages to be used, such as the ones designed by [30]. In our future

work, we can refer to the work of [16] to add the MIMO ambiguity function in the constraints of the radar waveform design so that not only the range and Doppler resolution but also the angular resolution could be enhanced.

Bibliography

[1] Mark A. Richards, James A. Scheer, and William A. Holm. *Principles of Modern Radar Volume I - Basic Principles*. SciTech Publishing, Inc., 2010.

[2] Jian Li, Luzhou Xu, Petre Stoica, Keith W. Forsythe, and Daniel W. Bliss. Range compression and waveform optimization for mimo radar: A CRB based study. *IEEE Transactions on Signal Processing*, 56(1):218–232, Jan 2008.

[3] Hao He, Petre Stoica, and Jian Li. Designing unimodular sequence sets with good correlations – including an application to MIMO radar. *IEEE Transactions on Signal Processing*, 57(11):4391–4405, Nov 2009.

[4] Jian Li, Petre Stoica, and Xumin Zhu. MIMO radar waveform synthesis. In *2008. RADAR '08. IEEE Radar Conference*, pages 1–6, May 2008.

[5] Yong-Chao Wang, Xu Wang, Hongwei Liu, and Zhi-Quan Luo. On the design of constant modulus probing signals for MIMO radar. *IEEE Transactions on Signal Processing*, 60(8):4432–4438, Aug 2012.

[6] Chun-Yang Chen. *Signal Processing Algorithms for MIMO Radar*. PhD thesis, California Institute of Technology , Pasadena, California, June 2009.

[7] Kritika Sengar, Nishu Rani, Ankita Singhal, Dolly Sharma, Seema Verma, and Tanya Singh. Study and capacity evaluation of SISO, MISO and MIMO RF wireless communication systems. *International Journal of Engineering Trends and Technology (IJETT)*, 9(9), May 2014.

[8] William L. Melvin and James A. Scheer. *Principles of Modern Radar Vol. II: Advanced Techniques*. SciTech Publishing, 2013.

[9] Keith W. Forsythe and Daniel W. Bliss. *MIMO Radar Signal Processing*, chapter 2, page 67. John Wiley & Sons, Inc., Hoboken, New Jersey, 2009.

[10] I. Oppermann and B.S. Vucetic. Complex spreading sequences with a wide range of correlation properties. *IEEE Transactions onCommunications*, 45(3):365–375, Mar 1997.

[11] P. Woodward. *Probability and Information Theory, with an Application to Radar*. Pergamon Press, 1957.

[12] M.R. Bell. Information theory and radar waveform design. *IEEE Transactions on Information Theory*, 39(5):1578–1597, Sep 1993.

[13] Yang Yang and R.S. Blum. MIMO radar waveform design based on mutual information and minimum mean-square error estimation. *IEEE Transactions on Aerospace and Electronic Systems*, 43(1):330–343, January 2007.

[14] Benjamin Friedlander. Waveform design for MIMO radars. *IEEE Transactions on Aerospace and Electronic Systems*, 43(3):1227–1238, July 2007.

[15] Yang Yang and R.S. Blum. Minimax robust MIMO radar waveform design. *IEEE Journal of Selected Topics in Signal Processing*, 1(1):147–155, June 2007.

[16] Chun-Yang Chen and P.P. Vaidyanathan. MIMO radar ambiguity properties and optimization using frequency-hopping waveforms. *IEEE Transactions on Signal Processing*, 56(12):5926–5936, Dec 2008.

[17] Petre Stoica, Jian Li, and Yao Xie. On probing signal design for MIMO radar. *IEEE Transactions on Signal Processing*, 55(8):4151–4161, Aug 2007.

[18] Yili Li and K.M. Wong. Riemannian distances for signal classification by power spectral density. *IEEE Journal of Selected Topics in Signal Processing*, 7(4):655–669, Aug 2013.

[19] D.R. Fuhrmann and G. San Antonio. Transmit beamforming for MIMO radar systems using signal cross-correlation. *IEEE Transactions on Aerospace and Electronic Systems*, 44(1):171–186, January 2008.

[20] Luzhou Xu, Jian Li, and Petre Stoica. Radar imaging via adaptive MIMO techniques. In *Proc. 14th Eur. Signal Process. Conf*, 2006.

[21] D.R. Fuhrmann and G. San Antonio. Transmit beamforming for MIMO radar systems using partial signal correlation. In *Proc. 38th Asilomar Conf. Signals, Systems, Computers*, volume 1, pages 295–299 Vol.1, Nov 2004.

[22] H.A. Khan, Yangyang Zhang, Chunlin Ji, C.J. Stevens, D.J. Edwards, and D. O'Brien. Optimizing polyphase sequences for orthogonal netted radar. *IEEE Signal Processing Letters*, 13(10):589–592, Oct 2006.

[23] Jorge Nocedal Stephen J. Wright. *Numerical Optimization*. Pringer Verlag, 1999.

[24] Petre Stoica, Hao He, and Jian Li. New algorithms for designing unimodular

sequences with good correlation properties. *IEEE Transactions on Signal Processing*, 57(4):1415–1425, April 2009.

[25] Jian Li, Petre Stoica, and Xiayu Zheng. Signal synthesis and receiver design for MIMO radar imaging. *IEEE Transactions on Signal Processing*, 56(8):3959–3968, Aug 2008.

[26] S. Boyd M. Grant and Y. Y. Ye. CVX: Matlab software for disciplined convex programming. Sept. 2012.

[27] J. L. Walsh. A closed set of normal orthogonal functions. *American Journal of Mathematics*, 45(1):5–24, Jan. 1923.

[28] K. Beauchamp. *Applications of Walsh and Related Functions: With an Introduction to Sequency Theory*. Academic Press Inc., Dec. 1984.

[29] A. Tchegho, S. Sattler, and H. Grab. Mixed-signal testing using Walsh functions. In *Mixed-Signals, Sensors, and Systems Test Workshop, 2009. IMS3TW '09. IEEE 15th International*, pages 1–8, June 2009.

[30] Q. Jin, Z. Luo, and K.M. Wong. An optimum complete orthonormal basis for signal analysis and design. *IEEE Transactions on Information Theory*, 40(3):732–742, May 1994.